DOI: 10.1002/chem.200500927

Orientational Effect of Aryl Groups on ^{77}Se NMR Chemical Shifts: Experimental and Theoretical Investigations

Waro Nakanishi,*[a] Satoko Hayashi,[a] Daisuke Shimizu,[a] and Masahiko Hada[b]

Dedicated to Prof. Michinori Ōki on occasion of his 77th birthday

Abstract: The orientational effect of *p*-YC_6H_4 (Ar) on δ(Se) is elucidated for ArSeR, based on experimental and theoretical investigations. The effect is examined in the cases in which Se−C_R in ArSeR is either in the Ar plane (pl) or is perpendicular to the plane (pd). 9-(Arylselanyl)anthracenes (**1**) and 1-(arylselanyl)anthraquionones (**2**) are employed to establish the effect in pl and pd, respectively. Large upfield shifts are observed for Y = NMe_2, OMe, and Me, and large downfield shifts for Y = COOEt, CN, and NO_2 in **1**, relative to Y = H, as is expected. Large upfield shifts are brought by Y = NMe_2, OMe, Me, F, Cl, and Br, and downfield shifts by Y = CN and NO_2 in **2**, relative to Y = H, with a negligible shift by Y = COOEt. Absolute magnetic shielding tensors of Se (σ(Se)) are calculated for ArSeR (R = H, Me, and Ph), assuming pl and pd, based on the DFT-GIAO method. Observed characters are well explained by the total σ(Se). Paramagnetic terms (σ^p(Se)) are governed by ($\sigma^p(Se)_{xx}+\sigma^p(Se)_{yy}$), in which the direction of n_p(Se) (constructed by $4p_z$(Se)) is set to the *z* axis. The main interaction in pl is the n_p(Se)–$\pi(C_6H_4)$–p_z(Y) type. The Y dependence in pl occurs through admixtures of $4p_z$(Se) in $\pi(SeC_6H_4Y)$ and π^*-(SeC_6H_4Y), modified by the conjugation, with $4p_x$(Se) and $4p_y$(Se) in σ-(CSeX) and σ^*(CSeX) (X = H or C) under a magnetic field. The main interaction in pd is the σ(CSeX)–$\pi(C_6H_4)$–p_x(Y) type, in which Se−X is nearly on the *x* axis. The Y dependence in pd mainly arises from admixtures of $4p_z$(Se) in n_p(Se) with $4p_x$(Se) and $4p_y$(Se) in modified σ^*(CSeX), since n_p(Se) is filled with electrons. It is demonstrated that the effect of Y on σ^p(Se) in the pl conformation is the same regardless of whether Y is an electron-donor or electron-acceptor, whereas for pd conformations the effect is greater when Y is an electron donor, as observed in **1** and **2**, respectively. Contributions of each molecular orbital and each transition on σ^p(Se) are evaluated, which enables us to recognize and visualize the effect clearly.

Keywords: ab initio calculations · aryl selenides · NMR spectroscopy · orientational effects · selenium · substituent effects

Introduction

^{77}Se NMR spectroscopy has been established as a powerful tools in the study of the selenium chemistry.[1] ^{77}Se NMR chemical shifts (δ(Se)) are sharply sensitive to the structural changes in selenium compounds. Therefore, they are widely applied to analyze the chemical bonds around Se atoms and/or to determine the structures.[2–5] While some empirical rules between structures and δ(Se) have been proposed,[2–5] it is not so easy to predict δ(Se) from the structures with substantial accuracy. The measurements of δ(Se) are necessary to understand based on plain rules founded on the theoretical background. A charge-transfer mechanism has been proposed to explain the downfield shift by the neighboring oxygen atom[6] and it is demonstrated that the mechanism plays an important role in weak interactions.[4] Other mecha-

[a] Prof. W. Nakanishi, Dr. S. Hayashi, D. Shimizu
Department of Material Science and Chemistry
Faculty of Systems Engineering, Wakayama University
930 Sakaedani, Wakayama 640–8510 (Japan)
Fax: (+81) 73-457-8253
E-mail: nakanisi@sys.wakayama-u.ac.jp

[b] Prof. M. Hada
Department of Chemistry
Faculty of Graduate School of Science
Tokyo Metropolitan University, 1–1 Minami-osawa
Hachioji-shi, Tokyo 192–0397 (Japan)

Supporting information for this article is available on the WWW under http://www.chemeurj.org/ or from the author.

 © 2006 Wiley-VCH Verlag GmbH & Co. KGaA, Weinheim

nisms must also be important when the structures are discussed based on the observed values. We have been much interested in the orientational effect on δ(Se) in *p*-YC_6H_4SeR (ArSeR), together with the mechanism. We have already pointed out the importance of the effect for the better interpretation of δ(Se) of ArSeR in a uniform manner.[5] A reliable guideline is necessary to determine the structures of selenium compounds based on δ(Se).

On the other hand, calculated absolute magnetic shielding tensors (σ) become reliable.[7] Although the contribution of relativistic terms has been pointed out for heavier atoms,[8] the perturbation would be small for the selenium nucleus. Therefore, the calculated tensors are useful for Se nuclei (σ(Se)) in common organic selenium compounds. As shown in Equation (1), the total absolute magnetic shielding tensor (σ^t) is decomposed into diamagnetic (σ^d) and paramagnetic (σ^p) contributions.[9] This decomposition includes small arbitrariness due to the coordinate origin dependence, though it does not damage our chemical analyses and insights into ^{77}Se NMR spectroscopy. The σ^p parameter contributes predominantly to σ^t in the structural changes seen in the selenium compounds. The magnetic shielding tensors consist of three components, which are exemplified by σ^p in Equation (2).

$$\sigma^t = \sigma^d + \sigma^p \quad (1)$$

$$\sigma^p = (\sigma^p_{xx} + \sigma^p_{yy} + \sigma^p_{zz})/3 \quad (2)$$

The parameters σ^p and σ^d are exactly expressed by the Ramsey's Equation,[10] and they are approximately calculated in the framework of the Hartree–Fock (HF) or DFT theory. Since σ^p is evaluated by the coupled Hartree–Fock (CPHF) method, they can be decomposed into the contribution of the occupied orbitals or the orbital–orbital transitions and are shown in Equation (3). The parameter σ^d is expressed simply as the sum of contributions over the occupied orbitals as shown in Equation (4).

$$\sigma^p = \sum_i^{occ} \sum_j^{unocc} \sigma^p_{i\rightarrow j} = \sum_i^{occ} \sigma^p_i \quad (3)$$

$$\sigma^d = \sum_i^{occ} \sigma^d_i \quad (4)$$

Based on the second-order perturbation theory at the level of the HF and single-excitation CI approximation, $\sigma^p_{i\rightarrow j}$ on a resonance nucleus *N* is shown to be proportional to reciprocal orbital energy gap ($\varepsilon_j - \varepsilon_i$), and expressed in Equation (5), in which ψ_k is the *k*th orbital function, $L_{z,N}$ is orbital angular momentum around the resonance nucleus, and r_N is the distance from the nucleus *N*.

$$\sigma^p_{zz,N} = -(\mu_o e^2/2\,m_e^2) \sum_i^{occ} \sum_j^{unocc} (\varepsilon_j - \varepsilon_i)^{-1} \times \{\langle\psi_i|L_z|\psi_j\rangle\langle\psi_j|L_{z,N} r_N^{-3}|\psi_i\rangle + \langle\psi_i|L_{z,N} r_N^{-3}|\psi_j\rangle\langle\psi_j|L_z|\psi_i\rangle\} \quad (5)$$

Consequently, while σ^p is evaluated accurately by the CPHF method and can be calculated by Equation (3), we will discuss σ^p with an approximated image derived from Equation (5). Since $\sigma^p_{zz,N}$ contains the $L_{z,N}$ operator, $\sigma^p_{zz,N}$ arises from admixtures between atomic p_x and p_y orbitals of *N* in various molecular orbitals. When a magnetic field is applied on a selenium compound, mixing of unoccupied molecular orbitals (ψ_j) into occupied molecular orbitals (ψ_i) will occur. Such admixtures generate $\sigma^p_{zz,N}$, if ψ_i and ψ_j contain p_x and p_y of *N*, for example. The parameters $\sigma^p_{xx,N}$ and $\sigma^p_{yy,N}$ are similarly understood.

It is useful to supply a series of δ(Se) of typical conformers in ArSeR, although conformers may change successively depending on the electronic and/or steric properties of R and Y.[11–13] Planar (pl) and perpendicular (pd) conformers will be discussed here, in which the Se–C_R bond in ArSeR is in the Ar plane in pl and perpendicular to the plane in pd. To clarify the relationship between the structures (conformers) and δ(Se), we tried to fix the conformers of all Ar groups in ArSeR examined. 9-(Arylselanyl)anthracenes (**1**: *p*-YC_6H_4SeAtc) and 1-(arylselanyl)anthraquinones (**2**: *p*-YC_6H_4SeAtq) were chosen as the candidates for pl and pd, respectively: Y in **1** and **2** are H (**a**), NMe_2 (**b**), OMe (**c**), Me (**d**), F (**e**), Cl (**f**), Br (**g**), COOEt (**h**), CN (**i**), and NO_2 (**j**). For the 9-anthryl (9-Atc) and 1-anthraquinonyl (1-Atq)

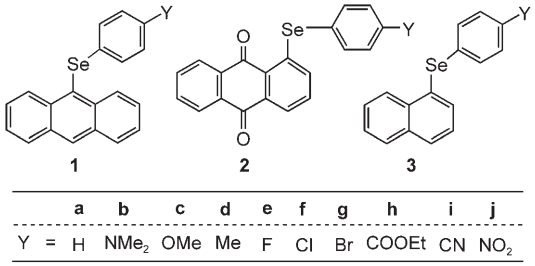

groups in **1** and **2**, respectively, as well as those proposed for 1-(arylselanyl)naphthalenes (**3**: *p*-YC_6H_4SeNap),[3e,4,11] the notation with A (perpendicular) B (parallel) and C (intermediate) conformations is used. The structure of **1** is A for 9-Atc and pl for Ar, which is denoted by **1**(A:pl). That of **2** is B for the 1-Atq and pd for Ar (**2**(B:pd)). The series of δ(Se) in **1** and **2** are typical for pl and pd, respectively.

To understand the orientational effect based on the theoretical background, quantum chemical (QC) calculations were performed on ArSeH (**4**), ArSeMe (**5**), and ArSePh (**6**). The conformations were fixed to pl and pd in the calculations. The gauge-independent atomic orbital (GIAO) method[14] was applied to evaluate σ(Se) at the DFT (B3LYP) level. Although the term $\sigma^p_{zz,Se}$ is used in Equation (5), $\sigma^p(Se)_{zz}$ will be used here on the analogy to δ(Se). Mechanisms of the orientational effect were explored for pl and pd, based on the magnetic perturbation theory. A utility program (NMRANAL-NH98G) was used

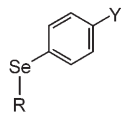

4 (R = H), **5** (R = Me), **6** (R = Ph)

 © 2006 Wiley-VCH Verlag GmbH & Co. KGaA, Weinheim

to carry out the decomposition of the magnetic shieldings, based on the Gaussian 98.[15] The program was also applied to evaluate the contributions separately from each molecular orbital (ψ_i) and each $\psi_i \rightarrow \psi_j$ transition, in which ψ_i and ψ_j denote occupied and unoccupied molecular orbitals, respectively. These results enabled us to evaluate and visualize the contributions.

Results and Discussion

Structures of 1c and 2a: Single crystals of **1c** and **2a** were obtained through slow evaporation of the samples in dichloromethane–hexane or benzene–hexane solvent mixtures. One of suitable crystals was subjected to X-ray crystallographic analysis for each compound. There are two types of structure in the crystal of **1c** (structure A and B). Only one type of structure corresponds to **2a** in the crystal. Figures 1 and 2 show structure A of **1c** (**1c**(S-A)) and the structure of **2a**, respectively.[16] The crystallographic data are collected in the Supporting Information.[17]

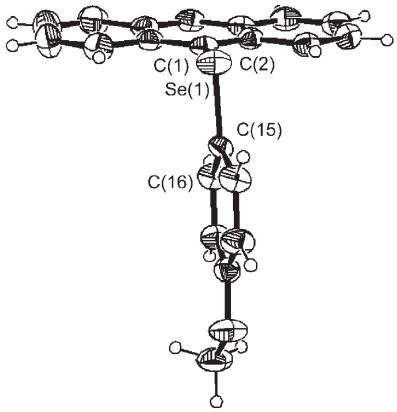

Figure 1. Structure of **1c**(S-A) (thermal ellipsoids are shown at 40% probability levels). Selected bond lengths (Å), angles (°), and torsional angles (°): Se(1)–C(1) 1.931(5), Se(1)–C(15) 1.925(5), C(1)-Se(1)-C(15) 99.4(2), C(2)-C(1)-Se(1)-(15) 95.6(4), C(1)-Se(1)-C(15)-C(16) 174.8(4).

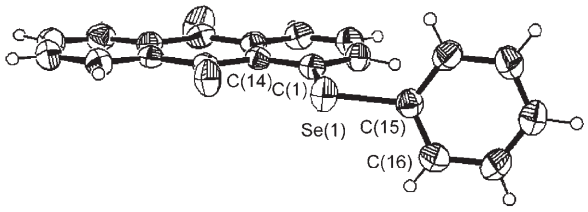

Figure 2. Structure of **2a** (thermal ellipsoids are shown at 40% probability levels). Selected bond lengths (Å), angles (°), and torsional angles (°): Se(1)–C(1) 1.921(3), Se(1)–C(15) 1.935(3), C(1)-Se(1)-C(15) 99.1(1), C(14)-C(1)-Se(1)-(15) 175.1(3), C(1)-Se(1)-C(15)-C(16) 87.7(3).

The planarity of the 9-Atc, 1-Atq, and Ar planes in **1c** and **2a** is very good. The Se(1)–C(15) bond of the *p*-anisylselanyl (*p*-AnSe) group in **1c**(S-A) is perpendicular to the 9-Atc plane (A) with the Se(1)–C(1) bond of 9-Atc being in the *p*-An plane (pl). The torsional angles of C(2)-C(1)-Se(1)-C(15) and C(1)-Se(1)-C(15)-C(16) in **1c**(S-A) are 95.6(4) and 174.8(4)°, respectively. The structure of **1c**(S-A) is very close to that of pure **1**(A:pl). On the other hand, the Se(1)–C(15) bond of the PhSe group in **2a** is in the 1-Atq plane (B) with the Se(1)–C(1) bond of 1-Atq being perpendicular to the Ph plane (pd). The torsional angles of C(14)-C(1)-Se(1)-C(15) and C(1)-Se(1)-C(15)-C(16) are 175.1(3) and 87.7(3)°, respectively. The structure of **2a** is very close to that of pure **2**(B:pd).

The structures of **1**(A:pl) and **2**(B:pd) are illustrated in Scheme 1, together with those of **3**. Why does **1c** have an (A:pl) structure? It must be the steric requirement of 9-Atc.

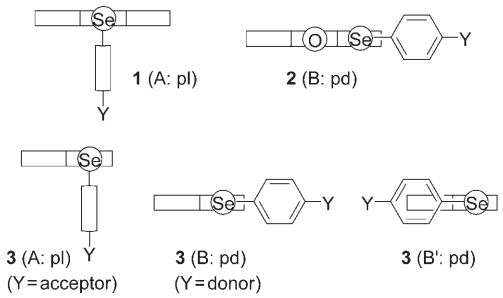

Scheme 1. Structures of **1** and **2**, together with those of **3**.

The structure of **1**(B:pd), which is similar to that of **3**(B′:pd), is unlikely to be stable.[18] The contribution of **1**(A:pd) must be considered, although **3**(A:pd) has not yet been observed. Compound **1**(A:pd) will be a transition state. QC calculations were performed on **1a**; as a result **1a**(A:pd) is predicted to be a transition state between **1a**(A:pl) and its duplicate (Scheme 2).[19] The activation energy of the internal rotation around the Se–C_{Ph} bond is evaluated to be 13.7 kJ mol^{-1} at 298 K. These results support that the global minimum of **1** is **1**(A:pl):[20] hence compound **1** will behave substantially as **1**(A:pl) in the solution.

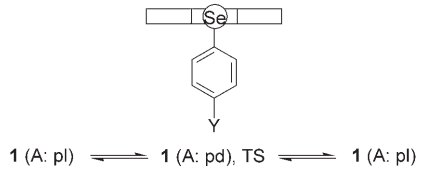

Scheme 2. Transition state nature of **1**(A:pd).

The structure of **2a** is (B:pd).[21] The nonbonded $n_p(O) \rightarrow \sigma^*(Se–C)$ three-center four-electron (3c-4e) type interaction operates in **2**(B:pd), which stabilizes the structure.[22,23] The **2**(B:pd) structure must also be stabilized by the p–π conjugation between $n_p(Se)$ and π orbitals of the Atq ring ($n_p(Se)$–π(Atq)). Consequently, **2**(B:pd) is stabilized by the energy lowering effect of the nonbonded O···Se–C 3c-4e in-

 © 2006 Wiley-VCH Verlag GmbH & Co. KGaA, Weinheim

teraction, together with the n_p(Se)–π(Atq) conjugation. The structure of all members of compounds of the **2** series is predicted to be (B:pd).[24]

^{77}Se NMR chemical shifts of 1 and 2: Table 1 shows the δ(Se) values for **1** and **2**[25] measured in [D]chloroform (0.050 M)[26] at 213, 297, and 333 K. The δ(Se) values of **1a** and **2a** are given relative to MeSeMe and those of **1b–j** and **2b–j** are given relative to **1a** and **2a**, respectively ($\delta(Se)_{SCS}$).

Table 1. Observed $\delta(Se)_{SCS}$ of **1** and **2** and calculated $\sigma^t_{rel}(Se)_{SCS}$ for **4–6** in pl and pd conformations.[a,b]

	T [K]	NMe_2 (**b**)	OMe (**c**)	Me (**d**)		H (**a**)	F (**e**)	Cl (**f**)	Br (**g**)	CO_2R[c] (**h**)[c]	CN (**i**)	NO_2 (**j**)
1	213	−22.7	−12.7	−6.3	0.0	(245.3)	−3.3	1.9	2.4	17.4	27.7	32.7
1	297	−21.0	−12.2	−6.6	0.0	(249.0)	−3.6	1.5	1.6	16.2	26.2	30.4
1	333	−21.3	−12.7	−6.8	0.0	(250.6)	−3.9	1.0	1.2	15.2	24.8	29.0
2	213	−20.6	−15.5	−9.2	0.0	(511.4)	−10.5	−7.1	−6.4	0.1	8.5	2.7
2	297	−19.6	−15.0	−9.0	0.0	(512.3)	−10.2	−7.1	−6.4	0.0	8.2	2.5
2	333	−19.5	−15.0	−9.1	0.0	(512.5)	−10.3	−7.2	−6.7	−0.3	7.9	2.2
4 (pl)		−36.4	−18.0	−8.2	0.0	(87.0)	−1.6	1.7	−1.8	14.3	29.8	33.7
5 (pl)		−23.9	−8.2	−8.0	0.0	(169.7)	2.1	4.7	7.2	24.6	29.7	43.8
6 (pl)		−20.5	−9.0	−3.7	0.0	(398.8)	1.1	1.9	2.3	13.1	20.2	28.6
4 (pd)		−35.9	−23.0	−15.6	0.0	(41.3)	−11.8	−9.1	−8.7	1.0	16.8	10.0
5 (pd)		−34.9	−21.2	−16.7	0.0	(219.1)	−14.1	−11.8	−12.6	3.0	13.4	6.6
6 (pd)		−34.2	−25.8	−14.6	0.0	(398.8)	−15.2	−13.3	−12.6	−3.4	7.0	0.5

[a] $\delta(Se)_{SCS}$ are given for **1** and **2**, together with δ(Se) for **1a** and **2a** in parenthesis, measured in [D]chloroform. [b] $\sigma^t_{rel}(Se)_{SCS}$ are given for **4–6**, together with σ^t_{rel}(Se) for **4a–6a** in parenthesis, calculated according to Equation (7) employing σ^i(Se:MeSeMe) = 1650.4 ppm. [c] R = Et for **1** and **2** and R = Me for **4–6**.

The values of δ(Se) of MeSeMe in [D]chloroform (10% v/v) shifts downfield by 5.6 ppm, if the frequency of the spectrometer is taken as the standard, when the temperature changes from 213 K to 333 K under the conditions.[27] The δ(Se) values of **1a**, **1b**, and **1j** move downfield by 5.3, 6.7, and 1.6 ppm, respectively, relative to MeSeMe, as the temperature changes from 213 K to 333 K. The results show that the temperature dependence of δ(Se) in **1a** and **1b** is roughly twice as large as that of MeSeMe, whereas the dependence in **1j** is comparable to that of MeSeMe.

To examine the temperature dependence in **1**, the δ(Se) values of **1** at 293 K and 333 K were plotted versus those at 213 K; excellent correlations ($r > 0.999$) were observed, see Table 2 (entries 1 and 2), in which the correlation constants (a) and the correlation coefficients (r) are given by Equation (6).

$$y = ax + b \; (r: \text{ correlation coefficient}) \tag{6}$$

The temperature dependence of **1** must be the reflection of the shallow energy surface in **1**(A:pl), resulting in the extended population to larger torsional angles of $\phi(C_9SeC_iC_o)$ around the energy minimum of $\phi = 0°$ at higher temperatures. The energy surfaces of Y with electron-donating groups must be shallower those with electron-accepting groups. The p–π conjugation of the n_p(Se)–π(C_6H_4Y-*p*) type affects on the stability of **1**(A:pl), in addition to the steric requirement of 9-Atc in **1**:[20] Y acceptors stabilize **1**(A:pl) more effectively than Y donors. The temperature dependence in $\delta(Se)_{SCS}$ for Y = OMe and NMe_2 seems complex, at a first glance. However, if we examine δ(Se) of **1b** and **1c**, relative to **1a**, we find them quite simple and monotonical. The characteristic temperature dependence of δ(Se) in **1a** may be responsible for the phenomenon.

Characteristic points of **1** are summarized as follows:

1) Large upfield shifts (−23 to −6 ppm) are observed for Y = NMe_2, OMe, and Me and large downfield shifts (17–33 ppm) for Y = COOEt, CN and NO_2, relative to Y = H.
2) A moderate upfield shift (−3 ppm) is observed for Y = F and small downfield shifts (2 ppm) for Y = Cl and Br.

Table 2. Correlations of δ(Se) for **1** and **2** and σ(Se) for **4–6**.[a]

	correlation	a	b	r	n
1	$\delta(Se:\mathbf{1})_{SCS,297K}$ vs. $\delta(Se:\mathbf{1})_{SCS,213K}$	0.940	−0.3	1.000	10
2	$\delta(Se:\mathbf{1})_{SCS,333K}$ vs. $\delta(Se:\mathbf{1})_{SCS,213K}$	0.916	−0.8	1.000	10
3	$\delta(Se:\mathbf{2})_{SCS,297K}$ vs. $\delta(Se:\mathbf{2})_{SCS,213K}$	0.957	−0.1	1.000	10
4	$\delta(Se:\mathbf{2})_{SCS,333K}$ vs. $\delta(Se:\mathbf{2})_{SCS,213K}$	0.946	−0.3	1.000	10
5	$\delta(Se:\mathbf{1})_{SCS,213K}$ vs. $\sigma^t_{rel}(Se:\mathbf{4}(pl))_{SCS}$	0.823	2.6	0.986	10
6	$\delta(Se:\mathbf{1})_{SCS,213K}$ vs. $\sigma^t_{rel}(Se:\mathbf{5}(pl))_{SCS}$	0.845	−2.1	0.990	10
7	$\delta(Se:\mathbf{1})_{SCS,213K}$ vs. $\sigma^t_{rel}(Se:\mathbf{6}(pl))_{SCS}$	1.218	−0.4	0.991	10
8	$\delta(Se:\mathbf{2})_{SCS,213K}$ vs. $\sigma^t_{rel}(Se:\mathbf{4}(pd))_{SCS}$	0.562	−1.5	0.990	10
9	$\delta(Se:\mathbf{2})_{SCS,213K}$ vs. $\sigma^t_{rel}(Se:\mathbf{5}(pd))_{SCS}$	0.599	−0.5	0.988	10
10	$\delta(Se:\mathbf{2})_{SCS,213K}$ vs. $\sigma^t_{rel}(Se:\mathbf{6}(pd))_{SCS}$	0.691	1.9	0.990	10
11	$\sigma^p(Se)$ vs. $(\sigma^p(Se)_{xx}+\sigma^p(Se)_{yy})$ in **4**(pl)	0.325	−583.7	1.000	22
12	$\sigma^p(Se)$ vs. $(\sigma^p(Se)_{xx}+\sigma^p(Se)_{yy})$ in **4**(pl)	0.357	−500.6	0.985	16[b]
13	$\sigma^p(Se)$ vs. $(\sigma^p(Se)_{xx}+\sigma^p(Se)_{yy})$ in **4**(pd)	0.335	−487.5	1.000	22
14	$\sigma^p(Se)$ vs. $(\sigma^p(Se)_{xx}+\sigma^p(Se)_{yy})$ in **4**(pd)	0.307	−553.4	0.998	16[b]
15	$\sigma^p(Se)$ vs. $(\sigma^p(Se)_{xx}+\sigma^p(Se)_{yy})$ in **5**(pl)	0.374	−442.0	0.998	14
16	$\sigma^p(Se)$ vs. $(\sigma^p(Se)_{xx}+\sigma^p(Se)_{yy})$ in **5**(pd)	0.345	−520.2	0.994	11[b]
17	$\sigma^p(Se)$ vs. $(\sigma^p(Se)_{xx}+\sigma^p(Se)_{yy})$ in **6**(pl)	0.309	−689.0	0.994	13
18	$\sigma^p(Se)$ vs. $(\sigma^p(Se)_{xx}+\sigma^p(Se)_{yy})$ in **6**(pd)	0.335	−598.8	0.999	10[b]
19	$\sigma^p(Se)_{yy}$ vs. $\sigma^p(Se)_{xx}$ in **4** (pd)	0.23	−455	0.85	16[b]
20	$\sigma^p(Se)_{yy}$ vs. $\sigma^p(Se)_{xx}$ in **5** (pd)	−0.33	−1722	0.93	14
21	$\sigma^p(Se)_{yy}$ vs. $\sigma^p(Se)_{xx}$ in **6** (pl)	−0.36	−2443	0.92	13
22	$\sigma^p(Se)_{yy}$ vs. $\sigma^p(Se)_{xx}$ in **6** (pd)	−0.65	−2721	0.95	13

[a] The constants a, b, r are defined in Equation (6) in the text. [b] For non-ionic species.

© 2006 Wiley-VCH Verlag GmbH & Co. KGaA, Weinheim

These charactistics must be the result of the **1**(A:pl) structure, in which n_p(Se) is parallel to the $\pi(C_6H_4Y\text{-}p)$. The set of δ(Se) of **1** can be used as a standard of pl.

In the case of **2**, the temperature dependence of δ(Se) is very small. The magnitude in compound **2a** is 1.1 ppm, relative to MeSeMe, under the temperature range from 213 K to 333 K. The plots of δ(Se) of **2** at 293 K and 333 K versus those at 213 K also give excellent correlations ($r > 0.999$). Table 2 collects the correlations (entries 3 and 4). The results show that **2**(B:pd) is thermally very stable and other conformers are negligible in the solution for all Y examined.

The character of δ(Se) in **2** is very different from that of **1**. Characteristic points of **2** are as follows:

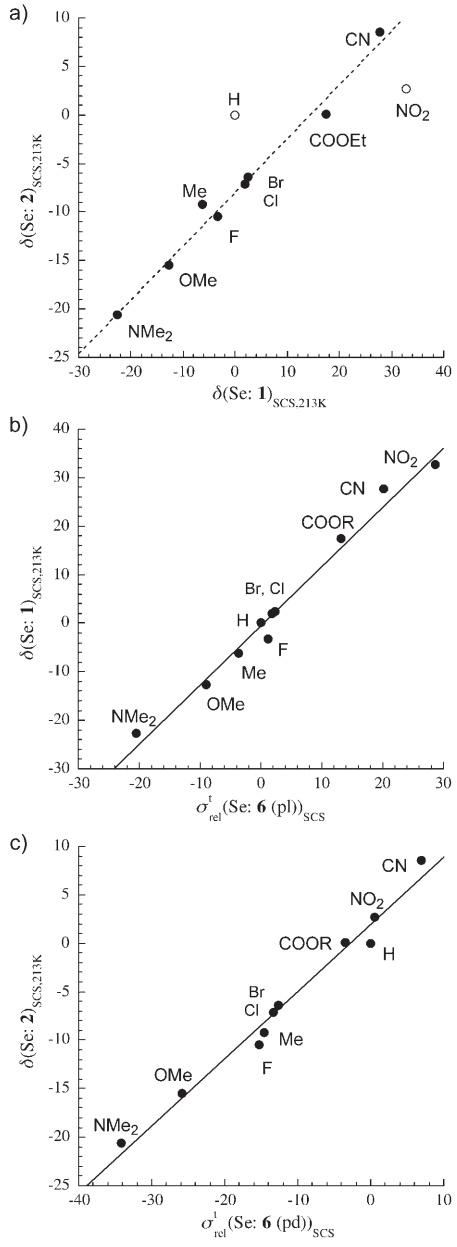

Figure 3. Plots of a) $\delta(Se:\mathbf{2})_{SCS,213K}$ versus $\delta(Se:\mathbf{1})_{SCS,213K}$, b) $\delta(Se:\mathbf{1})_{SCS,213K}$ versus $\sigma^t_{rel}(Se:\mathbf{6}(pl))_{SCS}$, and c) $\delta(Se:\mathbf{2})_{SCS,213K}$ versus $\sigma^t_{rel}(Se:\mathbf{6}(pd))_{SCS}$.

1) Large upfield shifts (−21 to −6 ppm) are observed for Y = NMe_2, OMe, Me, F, Cl, and Br, relative to Y = H.
2) Downfield shifts (3–9 ppm) are observed for Y = CN and NO_2, for which the magnitude with Y = CN is larger than that of NO_2, together with a negligible shift by Y = COOEt, relative to Y = H.

The characteristics must be the reflection of the **2**(B:pd) structure, in which n_p(Se) is perpendicular to $\pi(C_6H_4Y\text{-}p)$. The set of δ(Se) of **2** can be used as a typical standard of pd.

While $\delta(Se)_{SCS}$ of **1** is in a range of $-23 < \delta(Se)_{SCS} < 33$ ppm, that of **2** is $-21 < \delta(Se)_{SCS} < 9$ ppm. The Y donor and acceptor groups have an effect on $\delta(Se)_{SCS}$ of **1**, whereas only Y donor groups have an effect on the $\delta(Se)_{SCS}$ of **2**. The values of $\delta(Se)_{SCS}$ of **2** are plotted versus those of **1** in Figure 3a. Indeed, it emphasizes the difference in characters between **1** and **2**, but most of $\delta(Se)_{SCS}$ values of **2** seem to correlate well with those of **1**, as shown by a dotted line (a = 0.55). Two points corresponding to Y = H and NO_2 deviate from the line. Namely, δ(Se) of **2** with Y ≠ H are more upfield than those expected from δ(Se) of **1a** and **2a**, especially for **2j**.

Why is such peculiar behavior observed in **1** and **2**? Is it caused by the orientational effect of the aryl group? QC calculations were performed on **4–6**, assuming pl and pd for each, to elucidate the mechanism of the effect.

Observed δ(Se) of 1 and 2 versus calculated σ^t(Se) of 4–6: Scheme 3 shows axes and some orbitals of **4–6**, together with SeH_2. While the x axis in SeH_2 is in the bisected direction of ∠HSeH, the Se–H and Se–C bonds of MeSeH are almost on the x and y axes, respectively, although not shown. Axes of **4–6** are close to those in MeSeH in most cases. Since ∠CSeX (X = H or C) in **4–6** are close to 95, 98, and 101°, respectively, the bonds deviate inevitably from the axes to some extent. Axes are similar to those of SeH_2 for

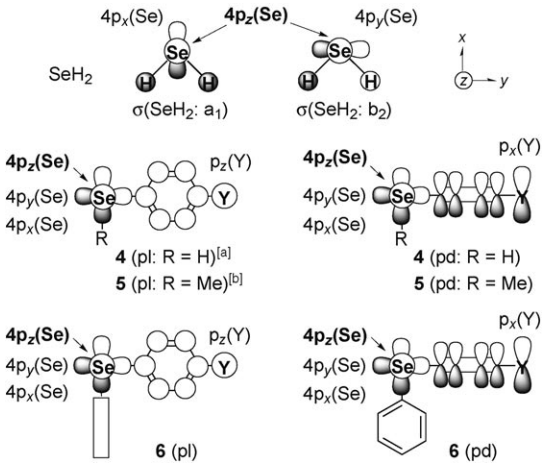

Scheme 3. Axes and some orbitals of **4–6**, together with those of SeH_2. [a] Axes with Y = Se^-, Br, and COOMe are close to those for SeH_2. [b] Axes with Y = Me, CN, and NH_3^+ are close to those for SeH_2.

 © 2006 Wiley-VCH Verlag GmbH & Co. KGaA, Weinheim

4(pl) with Y = Se^-, Br, and COOMe and **5**(pl) with Y = Me, CN, and NH_3^+ (Scheme 3).[28]

Structures of **4–6** in pl and pd and SeH_2 were optimized by employing the 6–311+G(3df) basis sets for Se and the 6–311+G(3d,2p) basis sets for other nuclei in the Gaussian 03 program.[29] Calculations are performed at the density functional theory (DFT) level of the Becke three-parameter hybrid functionals with the Lee–Yang–Parr correlation functional (B3LYP). Absolute magnetic shielding tensors of Se (σ(Se)) were calculated by the same method based on the DFT-GIAO method,[14] applying it to the optimized structures. Tables 3–5 give the σ^t(Se), σ^d(Se), σ^p(Se) parameters and the components, $\sigma^p(Se)_{xx}$, $\sigma^p(Se)_{yy}$, and $\sigma^p(Se)_{zz}$, for **4–6** bearing various substituents Y in pl and pd,[30] respectively.

It is instructive if σ^t(Se) of **4–6** in pl and pd can be compared directly with the observed δ(Se) of **1** and **2**. Relative shielding tensors of selenium compounds **S**, that is, **4–6** in pl and pd, σ^t_{rel}(Se:**S**), were calculated according to Equation (7), using σ^t(Se:MeSeMe) of 1650.4 ppm. The $\sigma^t_{rel}(Se:S)_{SCS}$ were also calculated similarly with the corresponding σ^t_{rel}(Se:**S**) values for **4–6** with Y = H in pl and pd. Table 1 also contains σ^t_{rel}(Se:**S**) values of **4–6** with Y = H and $\sigma^t_{rel}(Se:S)_{SCS}$ for **4–6**.

$$\sigma^t_{rel}(Se:\mathbf{S}) = -\{\sigma^t(Se:\mathbf{S}) - \sigma^t(Se:MeSeMe)\} \quad (7)$$

The characteristics observed for **1** and **2** are well explained by $\sigma^t_{rel}(Se)_{SCS}$. The $\delta(Se)_{SCS}$ values of **1** and **2** were plotted versus $\sigma^t_{rel}(Se)_{SCS}$ of ***n***(pl) and ***n***(pd) (***n*** = **4–6**). Good correlations were obtained and the results are given in Table 2 (entries 5–10). The *r* value for **1** becomes larger in an order of **4**(pl) < **5**(pl) ≈ **6**(pl) with *a* of **4**(pl) < **5**(pl) < **6**(pl). In the case of **2**, *r* becomes larger in an order of **5**(pd) < **4**(pd) ≈ **6**(pd) and *a* of **4**(pd) < **5**(pd) < **6**(pd). Figures 3b and c show the plots for **1** versus **6**(pl) and **2** versus **6**(pd), respectively. The results demonstrate that the characters of $\delta(Se)_{SCS}$ observed in **1** originate from the planar structure and those in **2** from the characteristic structure in which the Se–C_{Atq} bond in *p*-YC_6H_4SeAtq is perpendicular to the *p*-YC_6H_4 plane. The results are satisfactory, if we consider the limited experimental conditions and/or the different selenides employed in experimental study and in the calculations.

How does such an orientational effect arise from the structures? How does the electronic property of Y affect the δ(Se) values of **1** and **2**? The σ^p(Se) values of **4–6** are analyzed next.

Table 3. Calculated absolute shielding tensors (σ(Se)) of **4**, containing various Y.[a]

Y	σ^d(Se)	$\sigma^p(Se)_{xx}$	$\sigma^p(Se)_{yy}$	$\sigma^p(Se)_{zz}$	σ^p(Se)	σ^t(Se)
4(pl)						
H	2999.5	−1571.7	−1042.3	−1694.2	−1436.1	1563.4
O^-	3001.4	−1537.7	−803.3	−1674.3	−1338.4	1662.9
S^-	3004.1	−1560.7	−843.6	−1680.5	−1361.6	1642.4
Se^-	3007.3	−1745.3	−648.1	−1704.1	−1365.8	1641.4
NH_2	3000.9	−1741.2	−828.0	−1671.4	−1413.5	1587.3
NMe_2	3006.4	−1676.1	−862.4	−1681.4	−1406.7	1599.8
OH	3001.0	−1777.1	−824.9	−1673.0	−1425.0	1576.1
OMe	3004.7	−1823.5	−757.0	−1689.5	−1423.3	1581.4
Me	3002.4	−1760.2	−848.1	−1684.2	−1430.8	1571.6
F	3001.4	−1800.4	−833.2	−1675.7	−1436.4	1565.0
Cl	3003.8	−1777.8	−868.7	−1680.0	−1442.2	1561.7
Br	3008.7	−1883.4	−745.3	−1701.6	−1443.4	1565.2
$CHCH_2$	3005.3	−1849.6	−786.8	−1696.4	−1444.3	1561.0
COOH	3007.4	−1812.7	−882.1	−1699.3	−1464.7	1542.7
COOMe	3010.0	−1469.6	−1197.4	−1715.7	−1460.9	1549.1
BH_2	3001.5	−1846.4	−866.9	−1691.1	−1468.2	1533.3
CN	3002.1	−1829.1	−889.8	−1686.5	−1468.5	1533.6
CHO	3005.3	−1889.0	−819.9	−1697.2	−1468.7	1536.6
NO_2	3004.9	−1836.6	−905.8	−1683.2	−1475.2	1529.7
Se^+	3006.6	−2563.0	−976.0	−1659.3	−1732.8	1273.9
S^+	3003.7	−2579.3	−1292.6	−1650.6	−1840.9	1162.9
O^+	3000.5	−2680.8	−1600.0	−1647.7	−1976.2	1024.4
4(pd)						
H	3001.9	−1870.9	−869.9	−1437.6	−1392.8	1609.1
O^-	3002.6	−1547.6	−875.7	−1541.6	−1321.7	1680.9
S^-	3002.4	−1590.4	−868.2	−1507.8	−1322.1	1680.3
Se^-	2999.4	−1603.2	−866.2	−1495.2	−1321.5	1677.9
NH_2	3000.0	−1775.8	−861.7	−1451.5	−1363.0	1637.0
NMe_2	3004.1	−1782.2	−842.4	−1452.8	−1359.1	1645.0
OH	3001.4	−1793.9	−863.7	−1449.1	−1368.9	1632.5
OMe	3005.4	−1805.2	−871.3	−1443.6	−1373.4	1632.1
Me	3002.2	−1821.7	−871.0	−1439.8	−1377.5	1624.7
F	3000.8	−1829.8	−866.2	−1443.7	−1379.9	1620.9
Cl	3000.8	−1834.5	−870.2	−1442.8	−1382.5	1618.2
Br	3000.5	−1835.5	−870.5	−1442.1	−1382.7	1617.8
$CHCH_2$	3003.6	−1843.1	−876.7	−1438.7	−1386.2	1617.4
COOH	3006.1	−1880.4	−880.5	−1440.2	−1400.4	1605.7
COOMe	3004.2	−1872.6	−879.2	−1436.5	−1396.1	1608.1
BH_2	3001.5	−1889.4	−884.3	−1439.2	−1404.3	1597.2
CN	2999.9	−1901.0	−881.6	−1440.1	−1407.6	1592.3
CHO	3003.3	−1895.1	−884.4	−1438.1	−1405.9	1597.4
NO_2	3000.7	−1877.7	−884.4	−1442.8	−1401.6	1599.1
Se^+	2998.7	−1482.5	−45333.3	−1649.8	−16155.2	−13156.5
S^+	3000.2	−2941.4	295.6	−1657.9	−1434.6	1565.7
O^+	2999.2	−2821.1	−3947.0	−1713.4	−2827.2	172.0

[a] Structures were optimized with the 6–311+G(3df) basis sets for Se and 6–311+G(3d,2p) basis sets for other nuclei at the DFT (B3LYP) level, assuming pl and pd for each of Y. σ(Se) were calculated based on the DFT-GIAO method with the same basis sets.[29]

© 2006 Wiley-VCH Verlag GmbH & Co. KGaA, Weinheim

Table 4. Calculated absolute shielding tensors (σ(Se)) of **5**, containing various Y.[a]

Y	σ^d(Se)	$\sigma^p(Se)_{xx}$	$\sigma^p(Se)_{yy}$	$\sigma^p(Se)_{zz}$	σ^p(Se)	σ^i(Se)
5(pl)						
H	3006.5	−1893.4	−999.0	−1684.9	−1525.8	1480.7
O^-	3005.4	−1685.1	−1056.5	−1640.3	−1460.7	1544.7
COO^-	3008.7	−1544.2	−1236.7	−1676.3	−1485.7	1523.0
NMe_2	3007.7	−1645.4	−1194.5	−1669.5	−1503.1	1504.6
OMe	3007.4	−1741.5	−1136.8	−1677.1	−1518.4	1488.9
Me	3008.0	−1815.2	−1064.7	−1678.0	−1519.3	1488.7
F	3006.2	−1911.7	−990.8	−1680.6	−1527.7	1478.6
Cl	3006.7	−1639.8	−1269.8	−1682.4	−1530.7	1476.0
Br	3008.1	−1768.8	−1156.2	−1679.0	−1534.7	1473.5
COOMe	3009.6	−1840.5	−1132.8	−1687.1	−1553.5	1456.1
CN	3006.6	−1601.6	−1377.0	−1688.1	−1555.6	1451.0
BH_2	3006.9	−1892.9	−1110.2	−1683.2	−1562.1	1444.8
NO_2	3007.0	−1800.0	−1220.1	−1690.0	−1570.1	1436.9
NH_3^+	3006.9	−1771.0	−1401.0	−1709.6	−1627.2	1379.7
5(pd)						
H	2998.0	−1956.8	−1086.4	−1656.9	−1566.7	1431.3
O^-	3000.3	−1606.3	−1203.9	−1716.8	−1509.0	1491.3
COO^-	3002.2	−1766.1	−1152.4	−1640.9	−1519.8	1482.4
NMe_2	3003.5	−1889.2	−1062.0	−1660.9	−1537.3	1466.2
OMe	3004.1	−1938.6	−1059.6	−1656.6	−1551.6	1452.5
Me	2999.8	−1908.0	−1090.1	−1657.2	−1551.8	1448.0
F	2998.1	−1916.6	−1077.7	−1663.9	−1552.8	1445.4
Cl	2999.3	−1925.8	−1078.6	−1664.3	−1556.2	1443.1
Br	3001.0	−1930.0	−1077.7	−1663.5	−1557.1	1443.9
COOMe	3006.4	−2017.8	−1057.8	−1658.7	−1578.1	1428.3
CN	2998.0	−1995.5	−1076.6	−1668.2	−1580.1	1417.9
BH_2	2998.2	−1979.9	−1089.7	−1662.8	−1577.5	1420.7
NO_2	2999.5	−1977.4	−1075.9	−1671.0	−1574.7	1424.7
NH_3^+	2996.9	−2131.1	−1028.0	−1731.9	−1630.4	1366.5

[a] Structures were optimized with the 6–311+G(3df) basis sets for Se and 6–311+G(3d,2p) basis sets for other nuclei at the DFT (B3LYP) level, assuming pl and pd for each of Y. σ(Se) were calculated based on the DFT-GIAO method with the same basis sets.[29]

Evaluation of magnetic tensors based on molecular orbitals: Contributions of each molecular orbital (ψ_i) and each $\psi_i \rightarrow \psi_j$ transition on σ^p(Se) and the components, $\sigma^p(Se)_{xx}$, $\sigma^p(Se)_{yy}$, and $\sigma^p(Se)_{zz}$, are evaluated for **4a**, **5a**, **6a** (Y=H), and SeH_2, by using a utility program (NMRANAL-NH98G). The contributions were calculated in a similar manner as the tensors given in Tables 3–5, by the same method. The structures optimized with the Gaussian 03 program were employed for the evaluation. The directions of p_x(Se), p_y(Se), and p_z(Se) are shown in Scheme 3. The parameteres $\sigma^p(Se)_{xx}$, $\sigma^p(Se)_{yy}$, and $\sigma^p(Se)_{zz}$ arise from [p_y(Se); p_z(Se)], [p_z(Se); p_x(Se)], and [p_x(Se); p_y(Se)], respectively, in which [A; B] shows admixtures between atomic orbitals A and B, under a magnetic field [compare with Eq. (5)].

Table 6 contains the values of σ^p(Se), the components, and the contribution of each ψ_i, together with orbital energies and main character of Se in SeH_2.[31] Table 7 shows the contribution of each $\psi_i \rightarrow \psi_j$ transition on the $\sigma^p(Se)_{xx}$, $\sigma^p(Se)_{yy}$, and $\sigma^p(Se)_{zz}$ parameters, together with the energy differences of the transition and main character of Se in the molecular orbital ψ_j in SeH_2. Table 8 exhibits σ^p(Se), the components, and contributions of each ψ_i, together with the energies and main character of Se in **4a**–**6a**,[32] for which those of 4p(Se) and 4s(Se) are mainly shown for **4a** and those of 4p(Se) for **5a** and **6a**. Table 9 lists the contributions of each $\psi_i \rightarrow \psi_j$ transition for **4a**, together with the energy difference of each transition and main character of Se in the molecular orbital ψ_j.

Contributions of the p_z(Se) character in occupied ψ_i orbitals were evaluated.[33] The method is explained exemplified by SeH_2. The molecular orbitals ψ_{18}, ψ_{13}, ψ_9, and ψ_5 of SeH_2 have B1 symmetry. While ψ_{18}, ψ_9, and ψ_5 are mainly constructed from 4p_z(Se), 3p_z(Se), and 2p_z(Se), respectively, the character of ψ_{13} is 3d_{xz}(Se).[34] The four orbitals are assumed to have the p_z(Se) character here and are denoted collectively as "ψ_i". The $\sigma^p(Se)_{xx}$, $\sigma^p(Se)_{yy}$, $\sigma^p(Se)_{zz}$, and σ^p(Se) parameters are summed over "ψ_i". They are represented by $\sigma^p(Se)_{xx(zi)}$, $\sigma^p(Se)_{yy(zi)}$, $\sigma^p(Se)_{zz(zi)}$, and $\sigma^p(Se)_{(zi)}$, respectively, in which the suffix (*zi*) means the contribution of the p_z(Se) character in occupied "ψ_i". The results are given in Table 10, along with those for **4a**–**6a**.[35,36] The parameters $\sigma^p(Se)_{xx(zi)}$ and $\sigma^p(Se)_{yy(zi)}$ will be good approximations of the values from [p_z(Se) in ψ_i; p_y(Se) in ψ_j] and [p_z(Se) in ψ_i; p_x(Se) in ψ_j], respectively. The $\sigma^p(Se)_{zz(zi)}$ values are essentially zero, since they are related to [p_z(Se) in "ψ_i"; p_z(Se) in ψ_j]. Those from [p_x(Se) in "ψ_i"; p_y(Se) in ψ_j]+[p_y(Se) in "ψ_i"; p_x(Se) in ψ_j] are also essentially zero, since the p_x(Se) and p_y(Se) characters are negligible in "ψ_i".

Equation (8) defines $\sigma^p(Se)_{AA(xi'+yi')}$ ($A=x$, y, z, and zero), in which *i'* comes from "$\psi_{i'}$" that are ψ_i other than "ψ_i".[35] They correspond to the contributions of p_x and p_y in ψ_i to $\sigma^p(Se)_{AA}$.

$$\sigma^p(Se)_{AA(xi'+yi')} = \sigma^p(Se)_{AA} - \sigma^p(Se)_{AA(zi)} \quad (8)$$

The values are also shown in Table 10. The $\sigma^p(Se)_{xx(xi'+yi')}$ values result from the admixtures [p_x(Se) in ψ_i; p_x(Se) in ψ_j]+[p_y(Se) in ψ_i; p_z(Se) in ψ_j] and $\sigma^p(Se)_{yy(xi'+yi')}$ to [p_x(Se) in ψ_i; p_z(Se) in ψ_j]+[p_y(Se) in ψ_i; p_y(Se) in ψ_j]. The admixtures [p_x(Se) in ψ_i; p_x(Se) in ψ_j] and [p_y(Se) in ψ_i; p_y(Se) in ψ_j] are denoted by $\sigma^p(Se)_{xx(xi')}$ and $\sigma^p(Se)_{yy(yi')}$, respectively, which are essentially zero. Therefore, $\sigma^p(Se)_{xx(xi'+yi')}$ and $\sigma^p(Se)_{yy(xi'+yi')}$ would reduce to $\sigma^p(Se)_{xx(yi')}$ and $\sigma^p(Se)_{yy(xi')}$, respectively. The $\sigma^p(Se)_{zz(xi'+yi')}$ parameter is related to [p_x(Se) in ψ_i; p_y(Se) in ψ_j]+[p_y(Se) in ψ_i; p_x(Se) in ψ_j] admixtures.

After evaluation of σ^p(Se) and the components under the conditions, the next step is to elucidate the orientational

 © 2006 Wiley-VCH Verlag GmbH & Co. KGaA, Weinheim

Table 5. Calculated absolute shielding tensors (σ(Se)) of **6**, containing various Y.[a]

Y	σ^d(Se)	$\sigma^p(Se)_{xx}$	$\sigma^p(Se)_{yy}$	$\sigma^p(Se)_{zz}$	σ^p(Se)	σ^t(Se)
6(pl)						
H	2995.1	−1527.4	−1887.5	−1815.6	−1743.5	1251.6
O^-	2999.0	−1282.9	−2021.7	−1829.9	−1711.5	1287.5
COO^-	2999.3	−1379.1	−1953.6	−1840.6	−1724.5	1274.9
NMe_2	2997.7	−1462.8	−1902.3	−1811.6	−1725.5	1272.1
OMe	2995.5	−1504.1	−1887.4	−1813.2	−1734.9	1260.6
Me	2995.6	−1517.7	−1888.8	−1814.2	−1740.3	1255.3
F	2994.5	−1544.4	−1879.4	−1808.1	−1743.9	1250.5
Cl	2994.1	−1550.2	−1873.8	−1809.2	−1744.4	1249.7
Br	2996.5	−1553.1	−1871.1	−1817.4	−1747.2	1249.3
COOMe	2997.2	−1574.5	−1871.7	−1830.0	−1758.7	1238.5
CN	2994.8	−1605.6	−1869.2	−1815.6	−1763.5	1231.4
NO_2	2994.4	−1630.8	−1867.8	−1815.7	−1771.4	1223.0
NH_3^+	2992.1	−1786.8	−1835.6	−1804.9	−1809.1	1183.0
6(pd)						
H	2995.1	−1887.5	−1527.4	−1815.6	−1743.5	1251.6
O^-	2997.2	−1592.1	−1641.6	−1882.9	−1705.5	1291.6
COO^-	2999.3	−1733.0	−1601.5	−1815.2	−1716.6	1282.7
NMe_2	2998.3	−1787.3	−1531.6	−1818.6	−1712.5	1285.8
OMe	3002.2	−2044.1	−1313.9	−1816.4	−1724.8	1277.4
Me	2996.4	−1843.1	−1532.7	−1814.8	−1730.2	1266.2
F	2994.8	−1851.2	−1517.7	−1815.0	−1728.0	1266.8
Cl	2995.1	−1859.5	−1519.1	−1812.1	−1730.2	1264.9
Br	2997.2	−1871.4	−1514.8	−1812.8	−1733.0	1264.2
COOMe	3003.2	−2085.4	−1341.9	−1817.2	−1748.2	1255.1
CN	2998.5	−2132.1	−1310.6	−1818.8	−1753.8	1244.6
NO_2	2995.5	−1914.6	−1502.6	−1816.1	−1744.4	1251.1
NH_3^+	2992.2	−2043.9	−1437.0	−1848.7	−1776.5	1215.7

[a] Structures were optimized with the 6–311+G(3df) basis sets for Se and 6–311+G(3d,2p) basis sets for other nuclei at the DFT (B3LYP) level, assuming pl and pd for each of Y. σ(Se) are calculated based on the DFT-GIAO method with the same basis sets.[29]

Table 6. Contributions of each ψ_i on σ^p(Se) and the components in SeH_2, together with the energies and the main characters.[a]

i in ψ_i	ε [eV]	$\sigma^p(Se)_{xx}$	$\sigma^p(Se)_{yy}$	$\sigma^p(Se)_{zz}$	σ^p(Se)	*sym*	character
18	−6.91	−1334.9	−586.8	−0.4	−640.7	B1	$4p_z$(Se)
17	−9.86	−4.4	104.2	−333.9	−78.0	A1	$\sigma(4p_x(Se): a_1)$
16	−11.53	88.7	−15.1	−521.4	−149.3	B2	$\sigma(4p_y(Se): b_2)$
15	−19.58	−1.3	1.7	−16.2	−5.3	A1	σ(4 s(Se))
10–14	[b]	1.6	−1.2	6.6	2.3	[c]	3d(Se)
9	−156.63	−13.3	−7.8	0.0	−7.1	B1	$3p_z$(Se)
8	−156.85	0.0	2.1	−186.1	−61.3	A1	$\sigma(3p_x(Se): a_1)$
7	−156.95	−1.9	0.0	-8.1	−3.3	B2	$\sigma(3p_y(Se): b_2)$
6	−212.85	0.0	0.0	0.2	0.1	A1	3 s(Se)
5	−1418.53	4.3	5.9	0.0	3.4	B1	$2p_z$(Se)
4	−1418.60	0.0	−0.7	25.4	8.2	A1	$\sigma(2p_x(Se): a_1)$
3	−1418.63	−2.3	0.0	2.4	0.0	B2	$\sigma(2p_y(Se): b_2)$
1, 2	[d]	0.0	0.0	0.0	0.0	A1	1 s(Se), 2 s(Se)
1–18		−1263.6	−497.7	−1031.5	−930.9		

[a] Calculated using a utility program (NMRANAL-NH98G). [b] −57.65 to −57.33 eV. [c] Symmetries are B2, A1, A2, B1, and A1 for i=10–14, respectively. [d] −12350.82 and −1580.42 eV for i=1 and 2, respectively.

Analysis of σ^p(Se) in SeH_2: What admixtures cause the shifts in SeH_2? Contributions of each ψ_i and each $\psi_i \rightarrow \psi_j$ transition will answer the question. The ψ_{18} orbital (HOMO: n_p(Se)) of $4p_z$(Se) contributes −641 ppm to σ^p(Se) ($\sigma^p(Se)_{xx}$ = −1335 ppm and $\sigma^p(Se)_{yy}$ = −587 ppm), which is 69% of the total σ^p(Se) (Table 6). The $\psi_{18} \rightarrow \psi_{20}$ ($\sigma^*(SeH_2:b_2)$) transition is mainly responsible for $\sigma^p(Se)_{xx}$ (−1250 ppm) and $\psi_{18} \rightarrow \psi_{19}$ ($\sigma^*(SeH_2:a_1)$) and $\psi_{18} \rightarrow \psi_{24}$ ($\sigma^*(SeH_2: a_1')$) for $\sigma^p(Se)_{yy}$ (−511 ppm by the two; Table 7). ψ_{17} ($\sigma(SeH_2:a_1)$) and ψ_{16} ($\sigma(SeH_2:b_1)$) contribute −334 and −521 ppm, respectively, to $\sigma^p(Se)_{zz}$. While the $\psi_{17} \rightarrow \psi_{20}$ transition contributes −580 ppm to $\sigma^p(Se)_{zz}$; suitable transitions responsible for ψ_{16} cannot be found, other than the $\psi_{16} \rightarrow \psi_{24}$ transition ($\sigma^p(Se)_{zz}$ = −164 ppm). They must be spread over a wide range of ψ_j.

Contributions from the p_z(Se) character were also examined (Table 10). The $\sigma^p(Se)_{(zi)}$ value of −646 ppm corresponds to 69% of total σ^p(Se) and 99% of $\sigma^p(Se)_{(zi)}$ comes from ψ_{18}. Although $\sigma^p(Se)_{xx(zi)}$ (−1344 ppm), $\sigma^p(Se)_{yy(zi)}$ (−595 ppm), and $\sigma^p(Se)_{zz(xi'+yi')}$ (−1031 ppm) contribute much to the downfield shift, $\sigma^p(Se)_{xx(xi'+yi')}$ and $\sigma^p(Se)_{yy(xi'+yi')}$ contribute to the upfield shift. The results show that vacant orbitals containing the p_z(Se) character do not contribute to the downfield shift in SeH_2. After survey of SeH_2, next extension is to elucidate the orientational effect of **4**–**6**.

effect in **4**–**6**. Contributions by p_z(Se) in ψ_i will be discussed separately from those by p_x(Se) and p_y(Se) in ψ_i. The separation of contributions of p_x(Se) from those of p_y(Se) is also attempted, if possible. However, before we discuss the results for **4**–**6**, the σ^p(Se) values of SeH_2 will be surveyed first.[37,38]

Analysis of orientational effect in 4a–6a: The σ(Se) parameters of **4**–**6** are collected in Tables 3–5, respectively. The σ^p(Se) and σ^t(Se) of **4a**(pd) (Y=H) were evaluated to be larger (more upfield) than those of **4a**(pl) by 43 and 46 ppm, respectively; these shifts correspond to the orientational effect caused by Ph in **4a**.[39] The inverse orientational effect is predicted for **5a** (Y=H). The values of σ^p(Se) and σ^t(Se) of **5a**(pd) are smaller than those of **5a**(pl) by 41 and

 © 2006 Wiley-VCH Verlag GmbH & Co. KGaA, Weinheim

Table 7. Contributions of each $\psi_i \rightarrow \psi_j$ transition on $\sigma^p(Se)_{xx}$, $\sigma^p(Se)_{yy}$, and $\sigma^p(Se)_{zz}$ in SeH_2, together with the energy differences and characters of ψ_j.[a,b]

$\psi_i \rightarrow \psi_j$	$\Delta\varepsilon$ [eV]	$\sigma^p(Se)_{xx}$	$\sigma^p(Se)_{yy}$	$\sigma^p(Se)_{zz}$	character of ψ_j
18(B1)→19(A1)	6.28	0	−254	0	σ*(SeH_2: a_1)
18(B1)→20(B2)	6.67	−1250	0	0	σ*(SeH_2: b_2)
18(B1)→24(A1)	8.69	0	−257	0	σ*(SeH_2: a_1')
18(B1)→32(B2)	15.79	−138	0	0	[c]
17(A1)→20(B2)	9.62	0	0	−580	σ*(SeH_2: b_2)
17(A1)→32(B2)	18.74	0	−151	0	[c]
16(B2)→24(A1)	13.31	0	0	−164	σ*(SeH_2: a_1')
16(B2)→31(B1)	20.18	−124	0	0	σ*(SeH_2: b_2')

[a] Calculated using a utility program (NMRANAL-NH98G). [b] Values are shown if the magnitude of the total contribution, $|\sigma^p(Se)_{xx}+\sigma^p(Se)_{yy}+\sigma^p(Se)_{zz}|$, is larger than 120 ppm. [c] Would be $5p_z(Se)$.

49 ppm, respectively. While the values of $\sigma^p(Se)$ and $\sigma^t(Se)$ for **5a**(pl) are smaller than those of **4a**(pl) by 90 and 83 ppm, respectively, the values of **5a**(pd) are smaller than those of **4a**(pd) by 174 and 178 ppm, respectively. The differences are −84 and −95 ppm, respectively, which also correspond to the orientational effect of the Ph group in **5a** and **4a**. The more effective contribution to downfield shifts by the Se−C_{Me} bond in **5a**(pd), relative to **5a**(pl), must be responsible for the results.

The ψ_{38} orbital (HOMO) of $4p_z(Se)$-π_2 in **4a**(pl) contributes −220 ppm to $\sigma^p(Se)$ ($\sigma^p(Se)_{xx}=-454$ ppm and $\sigma^p(Se)_{yy}=-200$ ppm). The magnitude seems smaller than that expected from the p–π conjugation. The $\psi_{38}\rightarrow\psi_{41}$ (σ*(C_{Ph}SeH:b_2) transition is mainly responsible for $\sigma^p(Se)_{xx}$ (−325 ppm) and $\sigma^p(Se)_{yy}$ (−429 ppm). Although ψ_{36} and ψ_{32} also contain $4p_z(Se)$ and π(Ph) character, they contribute to upfield shifts. Instead, large downfield shifts are brought about by ψ_{35} of σ(C_{Ph}SeH:a_1) and ψ_{33} of σ(Se−H): the $\sigma^p(Se)$ value for ψ_{35} is −568 ppm ($\sigma^p(Se)_{xx}=-367$ ppm, $\sigma^p(Se)_{yy}=-217$ ppm, and $\sigma^p(Se)_{zz}=-1121$ ppm) and the $\sigma^p(Se)$ value for ψ_{33} is −515 ppm ($\sigma^p(Se)_{yy}=-767$ ppm and $\sigma^p(Se)_{zz}=-765$ ppm). The $\psi_{35}\rightarrow\psi_{41}$ and $\psi_{33}\rightarrow\psi_{41}$ transitions mainly contribute to $\sigma^p(Se)_{zz}$ with values of −1001 and −749 ppm, respectively. Typical transitions in **4a**(pl) are depicted in Figure 4a, which clarifies and visualizes the discussion.

As shown in Table 10, $\sigma^p(Se)_{xx(zi)}$, $\sigma^p(Se)_{yy(zi)}$, and $\sigma^p(Se)_{(zi)}$ of **4a**(pl) are −1305, 507, and −270 ppm, respectively. Although the main interaction in **4a**(pl) is the $p_z(Se)$–π(Ph) conjugation, $\sigma^p(Se)_{(zi)}$ of −270 ppm corresponds to only 19% of total $\sigma^p(Se)$, which is a striking contrast to the case of SeH_2. It must be the reflection of $\sigma^p(Se)_{yy(zi)}=507$ ppm. The large negative value of $\sigma^p(Se)_{yy(xi'+yi')}=-1553$ ppm demonstrates the substantial contribution of $p_z(Se)$ in π*(SePh) to the downfield shift in **4a**(pl).

In the case of **4a**(pd), a very large downfield shift is brought about by ψ_{38} (HOMO: $n_p(Se)$), which is constructed from almost pure $4p_z(Se)$.[40] Since ψ_{38} is filled with electrons, both $4p_x(Se)$ and $4p_y(Se)$ in σ*(C_{Ph}SeH) are expected to play a predominant role in the downfield shift. The expectation is demonstrated by the large negative values of $\sigma^p(Se)_{xx}$ (−1514 ppm) and $\sigma^p(Se)_{yy}$ (−468 ppm) in ψ_{38} (Table 8), together with $\sigma^p(Se)_{xx(zi)}=-1831$ ppm and $\sigma^p(Se)_{yy(zi)}=-602$ ppm (Table 10). The value of $\sigma^p(Se)_{xx(yi'+xi')}$ is 9 ppm, which is mainly produced from [$p_y(Se)$ in ψ_i; $p_z(Se)$ in ψ_j]. The results show that $p_z(Se)$ in vacant ψ_j contributes little in **4a**(pd), although $\sigma^p(Se)_{yy(yi'+xi')}$ is −316 ppm. Instead, $\sigma^p(Se)_{zz(yi'+xi')}$ (−1443 ppm) contributes to a large downfield shift, which must come from the various contributions of $4p_x(Se)$ and $4p_y(Se)$ in σ(C_{Ph}SeH) and σ*-(C_{Ph}SeH). The σ(C_{Ph}SeH)–π(Ph) interaction could contribute to the values in **4a**(pd). Typical transitions in **4a**(pd) are depicted in Figure 4b.

The $\sigma^p(Se)$ values of **5a** and **6a** are analyzed similarly. For **5a**(pl), the ψ_{42} (HOMO: $4p_z(Se)$-π_2) and ψ_{39} (σ($C_{Ph}SeC_{Me}$: a_1)) orbitals contribute large downfield shifts to $\sigma^p(Se)$, −363 and −857 ppm, respectively. The ψ_{42} (HOMO: $4p_z(Se)$) and ψ_{39} (σ($C_{Ph}SeC_{Me}$: a_1)) orbitals of **5a** (pd) contribute −591 and −593 ppm, respectively, to $\sigma^p(Se)$. The $\sigma^p(Se)_{(zi)}$ values of **5a** (pl) and **5a** (pd) are −769 and −833 ppm, respectively. The difference contributes to the orientational effect of **5a**. The more effective contribution by the Se−C_{Me} bond in **5a**(pd) to the downfield shifts than that in **5a**(pl) must be responsible for the effect.

In the case of **6a**, ψ_{58} (HOMO: $4p_z(Se)$-$\pi_{2(pl)}$) and ψ_{53} (σ($C_{Ph}SeC_{Ph}$: a_1)) contribute large downfield shifts to $\sigma^p(Se)$ with −631 and −1084 ppm, respectively. The $\sigma^p(Se)_{yy(zi)}$ (−1800 ppm), $\sigma^p(Se)_{xx(xi'+yi')}$ (−1309 ppm), and $\sigma^p(Se)_{zz(xi'+yi')}$ (−1805 ppm) components contribute greatly to downfield shifts, whereas $\sigma^p(Se)_{xx(zi)}$ (−6 ppm) is very small. The axes of **6a** were bisected in the Gaussian 98 program.[32]

What mechanism is operating in the Y dependence? The $\sigma^p(Se)$ of **4**–**6** in pl and pd are analyzed next.

Y dependence in 4–6: The Y dependence in **4**–**6** was examined employing $\sigma^p(Se)$ and the components in Tables 3–5. While $\sigma^p(Se)_{xx}$ and $\sigma^p(Se)_{yy}$ in **4**(pl) shift downfield and upfield by 200–300 ppm, respectively, when Y=H is replaced by Y=non-H,[41] those in **5**(pl) shift upfield and downfield by 100–200 ppm, respectively.[42] Such trend is not clear in **4**(pd), **5**(pd), and **6**.

To clarify the behavior of $\sigma^p(Se)$ in **4**(pl) and **4**(pd), $\sigma^p(Se)$ was plotted versus ($\sigma^p(Se)_{xx}+\sigma^p(Se)_{yy}$). Figures 5a and b exhibit the plots of $\sigma^p(Se)$ in **4**(pl) for all Y examined (containing anionic and cationic substituents) and that for Y of non-ionic groups, respectively. The correlation with all Y is very good and that with Y of non-ionic groups is also good.[43] The results are given in Table 2 (entries 11 and 12). The plot of $\sigma^p(Se)$ versus ($\sigma^p(Se)_{xx}+\sigma^p(Se)_{yy}$) for **4**(pd) gives a very good correlation for all Y;[43] this result may be due to a very wide range of $\sigma^p(Se)$ (entry 13).[44] Figure 5c shows a similar plot for **4**(pd) with Y being non-ionic groups. The correlation is very good and is given in Table 2 (entry 14).

 © 2006 Wiley-VCH Verlag GmbH & Co. KGaA, Weinheim

Table 8. Contributions of each ψ_i on σ^p(Se) and the components in **4a**–**6a**, together with the energies and the main characters.[a]

i in ψ_i	ε [eV]	$\sigma^p(Se)_{xx}$	$\sigma^p(Se)_{yy}$	$\sigma^p(Se)_{zz}$	σ^p(Se)	main character
4a(pl)						
38[b]	−6.08	−454.4	−199.6	−4.9	−219.6	$4p_z$(Se)-π_2
37	−7.29	3.5	−4.9	−3.3	−1.6	π_2'
36	−8.05	−509.3	643.9	−4.0	43.5	$4p_z$(Se)+π_2
35	−9.02	−366.9	−217.0	−1121.1	−568.3	σ(C_{Ph}SeH: a_1)
34	−9.80	0.2	−25.5	34.0	2.9	σ(Ph)
33	−10.28	−12.6	−766.9	−765.0	−514.8	σ(Se-H)
32	−10.53	−310.6	596.0	0.1	95.2	$4p_z$(Se)+π_1
31	−11.41	−32.9	−251.1	358.0	24.7	σ(C_{Ph}SeH: b_2)
1–38		−1572.3	−1046.1	−1696.8	−1438.4	
Δ[c]		0.0	0.0	0.0	0.0	
4a (pd)						
38[b]	−6.53	−1514.4	−468.3	−0.2	−661.0	$4p_z$(Se)
37	−7.28	3.1	−33.8	−263.8	−98.2	σ(Se-H)+π_2
36	−7.34	−4.5	−5.8	−0.5	−3.6	π_2'
35	−8.98	−124.1	−16.9	−791.6	−310.8	σ(C_{Ph}SeH: a_1)
34	−9.85	−79.7	−5.6	−0.2	−28.5	σ(Ph)
33	−10.04	−36.5	−104.0	−121.8	−87.4	σ(Se-H)-π_1
32	−10.76	60.4	−48.7	−245.5	−77.9	σ(Se-H)+π_1
31	−11.53	26.8	−68.8	198.1	52.0	σ(C_{Ph}SeH: b_2)
1–38		−1821.8	−917.9	−1439.8	−1393.2	
Δ[c]		−249.5	128.2	257.0	45.2	
5a(pl)						
42[b]	−5.75	−862.5	−222.3	−3.4	−362.7	$4p_z$(Se)-π_2
41	−7.17	−4.9	2.0	−3.4	−2.1	π_2'
40	−7.78	−596.5	104.4	−4.0	−165.4	$4p_z$(Se)+π_2
39	−8.60	−56.2	−490.2	−2023.6	−856.7	σ($C_{Ph}SeC_{Me}$: a_1)
38	−9.46	−143.8	−45.1	685.3	165.5	σ(Se-C_{Me})+σ(Ph)[d]
1–42		−1893.4	−999.0	−1684.9	−1525.8	
Δ[e]		0.0	0.0	0.0	0.0	
5a(pd)						
42[b]	−6.03	−1245.5	−525.8	−0.1	−590.5	$4p_z$(Se)
41	−7.14	−26.3	−26.1	−381.6	−144.7	σ(Se-C_{Me})+π_2
40	−7.26	−11.0	−5.8	−0.2	−5.7	π_2'
39	−8.56	−25.0	−200.2	−1553.7	−593.0	σ($C_{Ph}SeC_{Me}$: a_1)
38	−9.48	−310.8	42.6	917.5	216.4	σ(Se-C_{Me})+π(Ph)[d]
1–42		−1954.2	−1110.5	−1657.8	−1574.2	
Δ[e]		−60.8	−111.5	27.1	−48.4	
6a[f]						
58[b]	−5.82	−611.1	−1278.2	−3.2	−630.9	$4p_z$(Se)-$\pi_{2(pl)}$
57	−7.11	5.4	−2.9	−4.9	−0.8	$\pi_{2(pl)}'$
56	−7.32	−234.0	−16.3	−278.5	−176.2	σ($SeC_{Ph(pl)}$)-$\pi_{2(pd)}$
55	−7.41	−36.4	−21.1	1.2	−18.8	$\pi_{2(pd)}'$
54	−7.80	638.1	−267.0	−6.1	121.7	$4p_z$(Se)+$\pi_{2(pl)}$
53	−8.73	−954.5	−36.6	−2260.1	−1083.7	σ($C_{Ph(pl)}SeC_{Ph(pd)}$: a_1)
52	−9.29	24.7	−454.6	524.4	31.5	σ($C_{Ph(pl)}SeC_{Ph(pd)}$: b_2)
1–58		−1314.7	−2120.3	−1816.4	−1750.5	

[a] Calculated using a utility program (NMRANAL-NH98G). [b] Corresponding to HOMO. [c] σ^p(Se:**4a**(pl or pd))$_{AA}$−σ^p(Se:**4a**(pl))$_{AA}$, in which $A=x$, y, z, and zero. [d] Containing the σ($C_{Ph}SeC_{Me}$: b_2) character. [e] σ^p-(Se:**5a**(pl or pd))$_{AA}$−σ^p(Se:**5a**(pl))$_{AA}$, in which $A=x$, y, z, and zero. [f] Axes are in the bisected form in Gaussian 98.[32]

Points corresponding to Y=O$^-$, S$^-$, and Se$^-$ were also added in Figure 5c, although they deviate from the correlation. The correlation constants in entries 11–14 are 0.31–0.36, which are very close to one third (*cf*: Equation (2)). The results exhibit that the Y dependence of $\sigma^p(Se)_{zz}$ is negligible in **4** (see, Figure 6).[43] Namely, ($\sigma^p(Se)_{xx}+\sigma^p(Se)_{yy}$) effectively controls σ^p(Se) of **4**.

Similar trends in the Y dependence are also observed in **5** and **6**. The plots of σ^p(Se) versus ($\sigma^p(Se)_{xx}+\sigma^p(Se)_{yy}$) give good correlations both for **5**(pl) with all Y and **5**(pd) with Y of non-ionic groups (entries 15 and 16). Those of σ^p(Se) versus ($\sigma^p(Se)_{xx}+\sigma^p(Se)_{yy}$) in **6**(pl) with all Y and in **6** (pd) with Y of non-ionic groups are also very good (entries 17 and 18). The *a* values of 0.31–0.34 show that ($\sigma^p(Se)_{xx}+\sigma^p(Se)_{yy}$) control σ^p(Se) in **5** and **6**.[43]

The mechanism of the Y dependence can be elucidated in more detail, if $\sigma^p(Se)_{xx}$ and $\sigma^p(Se)_{yy}$ can be analyzed separately. To get an image in the behavior of $\sigma^p(Se)_{xx}$ and $\sigma^p(Se)_{yy}$, together with $\sigma^p(Se)_{zz}$, they are plotted versus σ^p(Se). Figure 6 shows the results for **4**(pd), **5**(pd), and **6**(pl). The correlations for **4**(pd) are linear and both $\sigma^p(Se)_{xx}$ and $\sigma^p(Se)_{yy}$ increase along with σ^p(Se). While $\sigma^p(Se)_{xx}$ and $\sigma^p(Se)_{yy}$ of **5**(pd) and **6**(pl) are on smooth lines, each slope for $\sigma^p(Se)_{yy}$ is the inverse of that for $\sigma^p(Se)_{xx}$. The slopes for $\sigma^p(Se)_{zz}$ are very small for all cases.[43]

$\sigma^p(Se)_{yy}$ was plotted versus $\sigma^p(Se)_{xx}$ for **4**–**6**. A fairly good correlation is obtained in the plot of **4**(pd) for Y of non-ionic groups with $a=0.23$ and $r=0.85$ (entry 19 in Table 2). The *a* value of 0.23 for **4**(pd) may indicate that the $4p_y$(Se) orbital involved in the Se–C_{Ar} bond is about four times more sensitive to the Y dependence than the $4p_x$(Se) orbital involved in the Se–H bond. The plot for **5**(pd) with all Y also gives a good correlation, but with a negative correlation constant, $a=-0.33$ and $r=0.93$ (entry 20). While the $4p_y$(Se) orbital involved in the Se–C_{Ar} bond of **5**(pd) contributes to the regular direction to σ^p(Se), the $4p_x$(Se) orbital involved in the Se–C_{Me} bond would work to shift to the inverse direction. Similar plots for **6**(pl) and **6**(pd) with all Y give good correlations, with $a=-0.36$ and $r=0.92$ (entry 21) and $a=-0.65$ and $r=0.95$ (entry 22), respectively. The $4p_y$(Se) orbital involved in the Se–C_{Ar} bond contributes to the regular direction in σ^p(Se), but the $4p_x$(Se) orbital in the Se–C_{Ph} bond seems to shift to the inverse direction both in **6**(pl) and **6**(pd). The re-

 © 2006 Wiley-VCH Verlag GmbH & Co. KGaA, Weinheim

Table 9. Contributions of each $\psi_i \rightarrow \psi_j$ transition on $\sigma^p(Se)_{xx}$, $\sigma^p(Se)_{yy}$, and $\sigma^p(Se)_{zz}$ in **4a**(pl) and **4a**(pl), together with the energy differences and the main characters of ψ_j.[a,b]

$\psi_i \rightarrow \psi_j$	$\Delta\varepsilon$ [eV]	$\sigma^p(Se)_{xx}$	$\sigma^p(Se)_{yy}$	$\sigma^p(Se)_{zz}$	character of ψ_j
4a(pl)					
38(A″)→41(A′)	5.43	−325	−429	0	σ*(C_{Ph}SeH: b_2)
38(A″)→42(A′)	5.97	−178	11	0	σ*(Se-C_{Ph})
38(A″)→43(A′)	6.29	−41	−116	0	σ*(C_{Ph}SeH: b_2')
38(A″)→51(A′)	8.06	−264	−17	0	σ*(C_{Ph}SeH: a_1)
36(A″)→41(A′)	7.40	−124	−163	0	σ*(C_{Ph}SeH: b_2)
35(A′)→41(A′)	8.37	0	0	−1001	σ*(C_{Ph}SeH: b_2)
35(A′)→43(A′)	9.23	0	0	−172	σ*(C_{Ph}SeH: b_2')
35(A′)→47(A″)	10.11	−46	−142	0	[c]
35(A′)→81(A″)	17.20	−135	−33	0	[d]
33(A′)→41(A′)	9.63	0	0	−749	σ*(C_{Ph}SeH: b_2)
33(A′)→42(A′)	10.16	0	0	137	σ*(Se-C_{Ph})
33(A′)→47(A″)	11.37	−20	−438	0	$5p_z$(Se)
33(A′)→51(A′)	12.25	0	0	−127	σ*(C_{Ph}SeH: a_1)
33(A′)→54(A′)	12.91	0	0	151	[d]
33(A′)→79(A′)	17.46	0	0	−128	[d]
4a(pd)					
38(A″)→41(A′)	6.18	−433	−264	0	σ*(C_{Ph}SeH: b_2)
38(A″)→42(A′)	6.43	−344	−48	0	σ*(C_{Ph}SeH)
38(A″)→43(A′)	6.80	−121	−200	0	σ*(C_{Ph}SeH: b_2)
38(A″)→45(A′)	7.37	−13	−116	0	σ*(Se-H)
38(A″)→48(A′)	7.85	−277	0	0	σ*(Se-C_{Ph})
38(A″)→53(A′)	8.90	−146	−16	0	[d]
35(A′)→41(A′)	8.63	0	0	−284	σ*(C_{Ph}SeH: b_2)
35(A′)→43(A′)	9.25	0	0	−175	σ*(C_{Ph}SeH: b_2)

[a] Calculated using a utility program (NMRANAL-NH98G). [b] Values are shown if the magnitude of the total contribution, $|\sigma^p(Se)_{xx}+\sigma^p(Se)_{yy}+\sigma^p(Se)_{zz}|$, is larger than 120 ppm. [c] Would be $5p_z$(Se). [d] Difficult to specify.

Table 10. Contributions of "ψ_i" and "$\psi_{i'}$" to $\sigma^p(Se)_{AA}$ ($A = x$, y, z, and zero) in **4a**–**6a**, together with SeH_2.[a]

ψ	$\sigma^p(Se)_{AA}$	x	y	z	zero
SeH_2					
ψ_1–ψ_{18}	$\sigma^p(Se)_{AA}$	−1264	−498	−1031	−931
"ψ_i"[b]	$\sigma^p(Se)_{AA(zi)}$	−1344	−595	0	−646
"$\psi_{i'}$"	$\sigma^p(Se)_{AA(xi'+yi')}$	80	97	−1031	−285
4a(pl)					
ψ_1–ψ_{38}	$\sigma^p(Se)_{AA}$	−1572	−1046	−1697	−1438
"ψ_i"[c]	$\sigma^p(Se)_{AA(zi)}$	−1305	507	−11	−270
"$\psi_{i'}$"	$\sigma^p(Se)_{AA(xi'+yi')}$	−267	−1553	−1686	−1168
4a(pd)					
ψ_1–ψ_{38}	$\sigma^p(Se)_{AA}$	−1822	−918	−1440	−1393
"ψ_i"[c]	$\sigma^p(Se)_{AA(zi)}$	−1831	−602	3	−810
"$\psi_{i'}$"	$\sigma^p(Se)_{AA(xi'+yi')}$	9	−316	−1443	−583
5a(pl)					
ψ_1–ψ_{42}	$\sigma^p(Se)_{AA}$	−1893	−999	−1685	−1526
"ψ_i"[c]	$\sigma^p(Se)_{AA(zi)}$	−1879	−413	−14	−769
"$\psi_{i'}$"	$\sigma^p(Se)_{AA(xi'+yi')}$	−14	−586	−1671	−757
5a(pd)					
ψ_1–ψ_{42}	$\sigma^p(Se)_{AA}$	−1954	−1110	−1658	−1574
"ψ_i"[c]	$\sigma^p(Se)_{AA(zi)}$	−1632	−865	−2	−833
"$\psi_{i'}$"	$\sigma^p(Se)_{AA(xi'+yi')}$	−322	−246	−1656	−741
6a[d]					
ψ_1–ψ_{58}	$\sigma^p(Se)_{AA}$	−1315	−2120	−1816	−1750
"ψ_i"[c]	$\sigma^p(Se)_{AA(zi)}$	−6	−1800	−11	−606
"$\psi_{i'}$"	$\sigma^p(Se)_{AA(xi'+yi')}$	−1309	−320	−1805	−1144

[a] Calculated using a utility program (NMRANAL-NH98G). [b] Belonging to the B1 symmetry. [c] Belonging to the A″ symmetry. [d] Axes are in the bisected form in Gaussian 98.[32]

sults are summarized in Scheme 4. The correlations are poor for **4**(pl) and **5**(pl).

Mechanism of Y dependence: The fact that $\sigma^p(Se)$ of **4**–**6** in pl and pd are effectively controlled by $(\sigma^p(Se)_{xx}+\sigma^p(Se)_{yy})$ lead us to elucidate the mechanisms of the Y dependence in the orientational effect, based on the magnetic perturbation theory. The mechanisms are explained exemplified by **4**(pl) and **4**(pd).

The main interaction between $4p_z$(Se) and p_z(Y) in **4**(pl) is the $4p_z$(Se)–π(C_6H_4)–p_z(Y) type of interaction, which modifies the contributions of $4p_z$(Se) in the π(SeC_6H_4Y) and π*(SeC_6H_4Y) molecular orbitals. Admixtures between $4p_z$(Se) in modified π-(SeC_6H_4Y) and π*(SeC_6H_4Y) molecular orbitals with $4p_y$(Se) and $4p_x$(Se) in σ(C_{Ar}SeH) and σ*(C_{Ar}SeH) molecular orbitals give rise to the Y dependence, when a magnetic field is applied. Consequently, when the Y subsitiutent is an electron donor or an electron acceptor, δSe of **4**(pl) depend on the substituent. The mechanism seems applicable to a wide range of Y (see, Figure 5a). In the case of **4**(pd), the $4p_z$(Se) orbital remains in n_p(Se) in the almost pure form.[40] The σ(C_{Ar}SeH)–π-(C_6H_4)–p_x(Y) interaction occurs instead; this interaction modifies the contributions of $4p_x$(Se) and $4p_y$(Se) orbitals in the σ-(C_{Ar}SeH) and σ*(C_{Ar}SeH) molecular orbitals. Admixtures of $4p_z$(Se) in n_p(Se) with $4p_y$(Se) and $4p_x$(Se) in modified σ*-(C_{Ar}SeH) mainly occur in **4**(pd), since n_p(Se) is filled with electrons. Namely, the Y dependence in **4** (pd) must be more sensitive to an electron-donating Y group; this result is in striking contrast to that of **4**(pl).

The mechanisms proposed for **4**(pl) and **4**(pd) are supported by the values found for $\sigma^p(Se)_{SCS}$. The $\sigma^p(Se)_{SCS}$ values for **4**(pl) are in an order of $Y = NO_2$ (−39.1) < CN (−32.4) < F (−0.3) ≈ H (0.0) < Me (5.3) < NMe_2 (29.4 ppm) and those for **4**(pd) are Y = CN (−14.8) < NO_2 (−8.8) < H (0.0) < F

 © 2006 Wiley-VCH Verlag GmbH & Co. KGaA, Weinheim

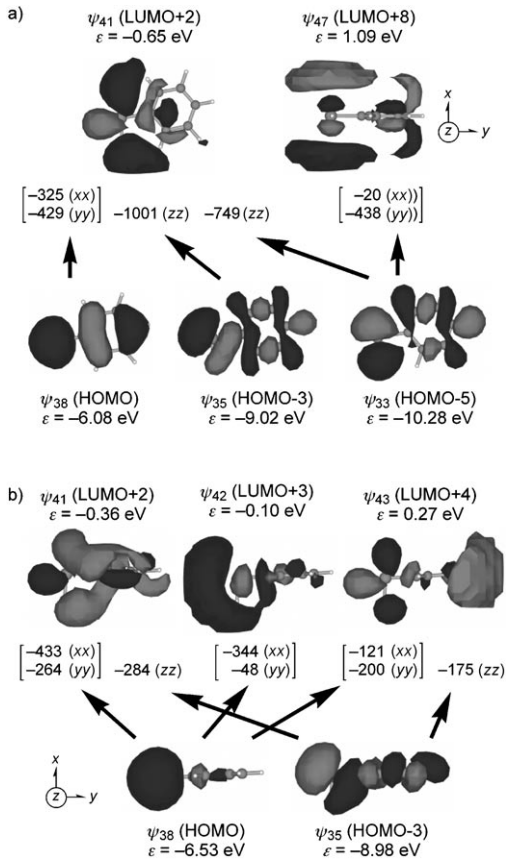

Figure 4. Contribution of each $\psi_i \rightarrow \psi_j$ transition to σ^p(Se): a) for **4a**(pl) and b) for **4a**(pd).

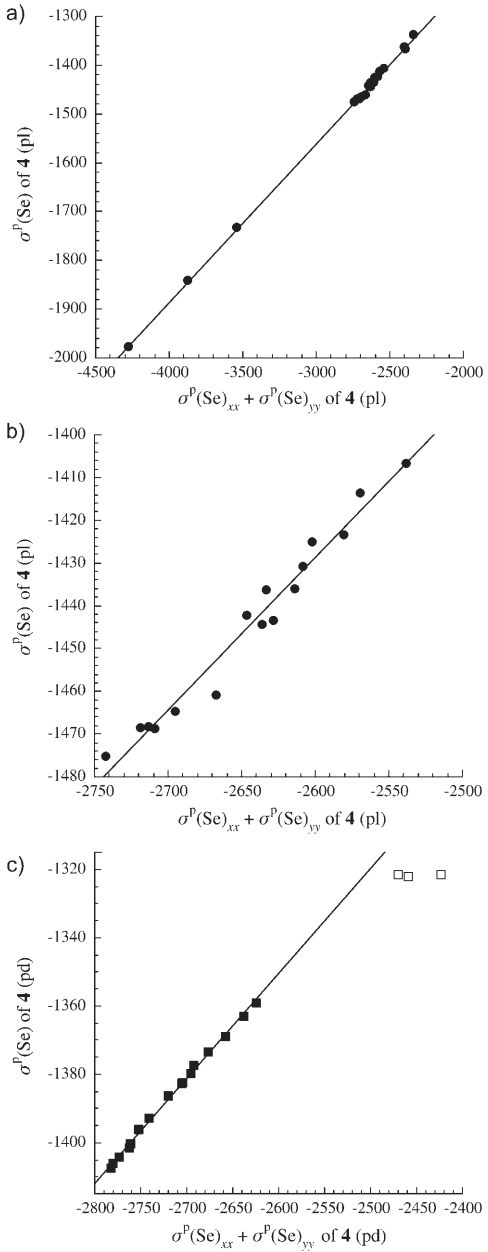

Figure 5. Plots of σ^p(Se) versus $\sigma^p(Se)_{xx}+\sigma^p(Se)_{yy}$: a) For **4**(pl) with all Y, b) for **4**(pl) with Y of non-ionic groups, and c) for **4**(pd) with Y of non-ionic groups (■), together with Y of anionic groups (□).

$(12.9) < Me\ (15.3) < NMe_2$ (33.7 ppm). It is demonstrated that both electron-donating and electon-accepting Y moieties contribute effectively to $\sigma^p(Se)_{SCS}$ in **4**(pl), whereas electron-donating Y groups are more effective than electron-accepting groups in **4**(pd). The predictions made for **4**(pl) and **4**(pd) are observed in **1** and **2**, respectively. Similar mechanisms must operate for **5** and **6**.

Details of the mechanism seem complex, since the contributions of $Y = NO_2$ and CN are different in **4**(pl) and **4**(pd). To clarify the mechanisms in more detail, the $\sigma^p(Se)_{(zi)SCS}$ values for **4**(pl) and **4**(pd) were evaluated for $Y = NH_2$, Me, F, CN, and NO_2, in addition to Y = H, by summarizing σ^p(Se) over "ψ_i".[35] The $\sigma^p(Se)_{(xi'+yi')SCS}$ values were also calculated according to Equation (8). The results are collected in Table 11. The signs of the $\sigma^p(Se)_{(zi)SCS}$ values are for most cases the same as those found for $\sigma^p(Se)_{SCS}$. The $\sigma^p(Se)_{SCS}$ parameters are roughly controlled by $\sigma^p(Se)_{(zi)SCS}$ and improved numerically by $\sigma^p(Se)_{(xi'+yi')SCS}$ both for **4**(pl) and **4**(pd). The magnitudes of $\sigma^p(Se)_{(zi)SCS}$ and $\sigma^p(Se)_{(xi'+yi')SCS}$ are less than 90 ppm, except for **4**(pl: $Y = NO_2$) for which values of 500 ppm are found; this result must be a reflection of the good electron-accepting character and the ability to extend π-systems. However, it is noteworthy that the total effect by NO_2 fits almost in the range of the substituents. The orientational effect, together with the mechanism of Y dependence, is well established based on the experimental and theoretical investigations.

Conclusion

The orientational effect is empirically established by the Y dependence on δ(Se) of **1** and **2**. The sets of δ(Se) of **1** and **2** can be used as the standards for pl and pd, respectively, when δ(Se) of aryl selenides are analyzed. The Y dependence observed in **1** and **2** is well explained by analyzing the

 © 2006 Wiley-VCH Verlag GmbH & Co. KGaA, Weinheim

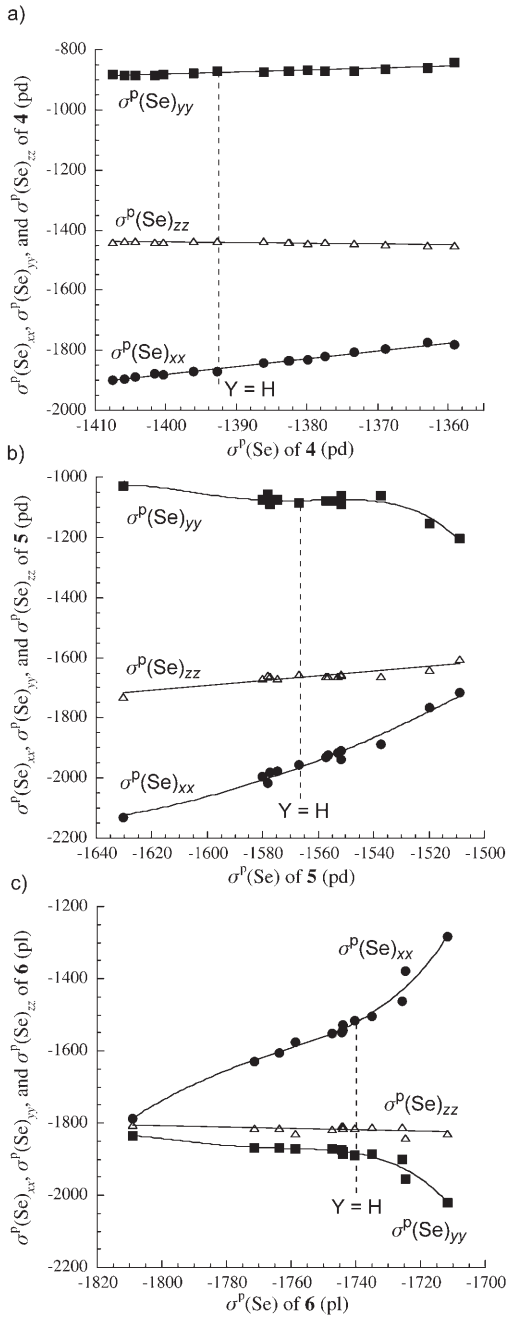

Figure 6. Plots of $\sigma^P(Se)_{xx}$ (●), $\sigma^P(Se)_{yy}$ (■), and $\sigma^P(Se)_{zz}$ (△) versus $\sigma^P(Se)$: a) for **4**(pd) with Y of non-ionic groups, b) for **5**(pd) with all Y, and c) for **6**(pl) with all Y.

σ^i(Se) values of **6**(pl) and **6**(pd), respectively, calculated with the DFT-GIAO method. While σ^i(Se) of **4a**(pl) is predicted to be more negative than that of **4a**(pd) by 46 ppm, σ^i(Se) of **5a**(pl) is evaluated to be larger than that of **5a**(pd) by 49 ppm. The differences correspond to the orientational effect of the Ph group in **4a** and **5a**.

Very good correlations are obtained in the plots of $\sigma^P(Se)$ versus $(\sigma^P(Se)_{xx}+\sigma^P(Se)_{yy})$ for **4**–**6** in pl and pd. Since the correlation constants (*a*) are very close to one third, $\sigma^P(Se)_{zz}$ must be almost constant when Y is changed. Consequently,

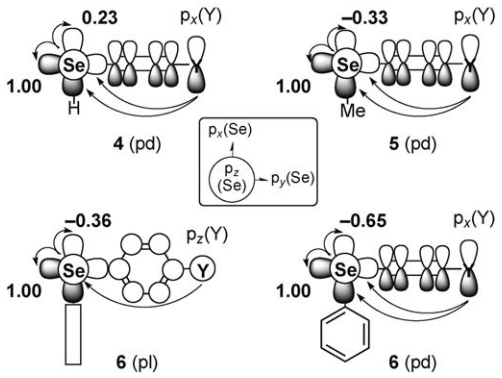

Scheme 4. Contributions of $\sigma^P(Se)_{yy}$ relative to $\sigma^P(Se)_{xx}$ in **4**–**6**, in which the contribution of each $\sigma^P(Se)_{xx}$ is taken to be 1.00. Contributions are depicted by reducing to p_x(Se) and p_y(Se), respectively.

we have demonstrated that $(\sigma^P(Se)_{xx}+\sigma^P(Se)_{yy})$ effectively control $\sigma^P(Se)$ of **4**–**6** in pl and pd. The results allowed us to elucidate the mechanisms of the Y dependence in the orientational effect, based on the magnetic perturbation theory. The main interaction in pl is the $n_p(Se)$–$\pi(C_6H_4)$–$p_z(Y)$ conjugation. Therefore, the Y dependence in pl occurs through admixtures of $4p_z(Se)$ in modified $\pi(SeC_6H_4Y)$ and $\pi^*(SeC_6H_4Y)$ molecular orbitals with $4p_x(Se)$ and $4p_y(Se)$ in $\sigma(CSeX)$ and $\sigma^*(CSeX)$ molecular orbitals (X = H or C). The main interaction in pd is the $\sigma(CSeX)$–$\pi(C_6H_4)$–$p_x(Y)$ interaction, which modifies both $\sigma(C_{Ar}SeH)$ and $\sigma^*(C_{Ar}SeH)$ molecular orbitals. The Y dependence in pd mainly originates from admixtures of $4p_z(Se)$ in the $n_p(Se)$ orbital with $4p_x(Se)$ and $4p_y(Se)$ in modified $\sigma^*(CSeX)$ molecular orbitals, since $n_p(Se)$ is filled with electrons. Consequently, both elctron-donating and electron-accepting Y moieties are effective in pl, whereas electron-donating Y moieties must be more effective in pd. The predictions for pl and pd are observed in **1** and **2**, respectively. Contributions of each molecular orbital and each transition on $\sigma^P(Se)$ have been evaluated, which enables us to recognize and visualize the effect clearly.

The effect of R in ArSeR is also important, which will be discussed elsewhere, together with the applications of the method.

Experimental Section

General considerations: Manipulations were performed under a nitrogen or an argon atmosphere with standard vacuum-line techniques. Glassware was dried at 130 °C overnight. Solvents and reagents were purified by standard procedures as necessary. Melting points were uncorrected. NMR spectra were recorded at 25 °C on a JEOL JNM-AL 300 spectrometer (^{1}H, 300 MHz; ^{13}C, 75.45 MHz; ^{77}Se, 57.25 MHz). The ^{1}H, ^{13}C, and ^{77}Se chemical shifts are given in ppm relative to those of Me_4Si, internal $CDCl_3$ in the solvent, and external MeSeMe, respectively. Column chromatography was performed on silica gel (Fuji Silysia BW-300), acidic alumina, and basic alumina (E. Merk). Flash column chromatography was performed with 300–400 mesh silica gel, acidic alumina, and basic alumina and analytical thin-layer chromatography was performed on precoated

 © 2006 Wiley-VCH Verlag GmbH & Co. KGaA, Weinheim

Table 11. Contributions of "ψ_i" and "$\psi_{\bar{i}}$" to $\sigma^p(Se)_{SCS}$ in some **4**(pl) and **4**(pd) for different Y substituents.[a]

	NO_2	CN		H	F	Me	NH_2
4(pl)							
$\sigma^p(Se)_{SCS}$	−33[b]	−34	0	(−1438)	0	8	23
$\sigma^p(Se)_{(z\bar{z})SCS}$	−478	−85	0	(−270)	−3	21	87
$\sigma^p(Se)_{(x\bar{x}+y\bar{y})SCS}$	445	51	0	(−1168)	3	−13	−64
4(pd)							
$\sigma^p(Se)_{SCS}$	−9	−15	0	(−1393)	11	15	18
$\sigma^p(Se)_{(z\bar{z})SCS}$	−64	−42	0	(−810)	−10	6	53
$\sigma^p(Se)_{(x\bar{x}+y\bar{y})SCS}$	55	27	0	(−583)	21	9	−35

[a] Calculated using a utility program (NMRANAL-NH98G). [b] About 6 ppm upfield relative to that derived from Table 3.

silica gel plates (60F-254) with the systems (v/v) indicated. Elemental analyses were performed using a J-Science Lab Co., JM10 Micro Corder.

Preparation of 9-(phenylselanyl)anthracene (1a): Under an argon atmosphere, 9-bromoanthracene (1.00 g, 3.89 mmol) was dissolved in dry diethyl ether (70 mL) and the solution was added to a flask that contained magnesium (0.10 g, 4.11 mmol) and dry diethyl ether (10 mL). The solution was refluxed for 2 h. A solution of diphenyl diselenide (1.21 g, 3.89 mmol) in diethyl ether (30 mL) was then added. Then the reaction mixture was refluxed for 1 h. Then, 5% hydrochloric acid (20 mL) and benzene (100 mL) were added. The organic layer was separated and then washed with brine, 10% aqueous solution of sodium hydroxide, saturated aqueous solution of sodium bicarbonate, and brine again. Then the solution was dried over sodium sulfate, evaporated, and dried in vacuo. The crude product was purified by column chromatography (SiO_2, hexane). Compound **1a** was isolated in 65% yield as yellow needles. M.p. 100.8–101.3 °C; ^{1}H NMR (300 MHz, $CDCl_3$, TMS): δ = 7.01–7.09 (m, 5H), 7.45–7.54 (m, 4H), 8.02 (dd, J = 2.6, 7.1 Hz, 2H), 8.56 (s, 1H), 8.87 ppm (dd, J = 0.8, 7.6 Hz, 2H); ^{13}C NMR (75 MHz, $CDCl_3$, TMS): δ = 125.5, 125.7, 127.1, 128.3, 128.8, 129.0, 129.1 (^3J(Se,C) = 3.1 Hz), 129.4 (^2J(Se,C) = 9.5 Hz), 130.2 131.9, 133.6, 135.1 ppm (^3J(Se,C) = 5.6 Hz); ^{77}Se NMR (57 MHz, $CDCl_3$, MeSeMe): δ = 249.0 ppm; elemental analysis calcd (%) for $C_{20}H_{14}Se$: C 72.07, H 4.23; found: C 72.33, H 4.15.

Preparation of 9-[(*N*,*N*'-dimethylamino)phenylselanyl]anthracene (1b): A similar method to that desribed for the preparation of **1a** was used. Compound **1b** was isolated in 82% yield as yellow needles. M.p. 168.3–170.7 °C; ^{1}H NMR (300 MHz, $CDCl_3$, TMS): δ = 2.80 (s, 6H), 6.45 (d, J = 9.0 Hz, 2H), 7.15 (d, J = 9.0 Hz, 2H), 7.47 (dt, J = 1.3, 6.6 Hz, 2H), 7.53 (dt, J = 1.6, 6.6 Hz, 2H), 7.99 (dd, J = 1.5, 8.1 Hz, 2H), 8.51 (s, 1H), 9.01 ppm (dd, J = 1.1, 9.0 Hz, 2H); ^{13}C NMR (75 MHz, $CDCl_3$, TMS): δ = 40.4, 113.4, 118.4, 125.3, 126.8, 128.8, 129.0, 129.5, 129.8 (^3J(Se,C) = 10.0 Hz), 131.9 (^2J(Se,C) = 12.4 Hz), 134.9 (^3J(Se,C) = 5.2 Hz), 149.3 ppm; ^{77}Se NMR (57 MHz, $CDCl_3$, MeSeMe): δ = 228.0 ppm; elemental analysis calcd (%) for $C_{22}H_{19}NSe$: C 70.21, H 5.09, N 3.72; found: C 70.26, H 5.10, N 3.70.

Preparation of 9-(anisylselanyl)anthracene (1c): A similar method to that desribed for the preparation of **1a** was used. Compound **1c** was isolated in 67% yield as yellow needles. M.p. 121.4–122.0 °C; ^{1}H NMR (300 MHz, $CDCl_3$, TMS): δ = 3.66 (s, 3H), 6.63 (d, J = 8.8 Hz, 2H), 7.11 (d, J = 9.0 Hz, 2H), 7.49 (dt, J = 1.5, 6.6 Hz, 2H), 7.46–7.58 (m, 2H), 8.02 (dd, J = 1.8, 7.9 Hz, 2H), 8.55 (s, 1H), 8.95 ppm (ddd, J = 1.3, 2.6, 8.8 Hz, 2H); ^{13}C NMR (75 MHz, $CDCl_3$, TMS): δ = 55.2, 114.9, 123.5, 125.4, 127.0, 128.0, 128.9, 129.6 (^3J(Se,C) = 10.0 Hz), 129.9, 131.4 (^2J(Se,C) = 12.4 Hz), 131.9, 134.9 (^3J(Se,C) = 5.2 Hz), 158.3 ppm; ^{77}Se NMR (57 MHz, $CDCl_3$, MeSeMe): δ = 236.8 ppm; elemental analysis calcd (%) for $C_{21}H_{16}OSe$: C 69.42, H 4.44; found: C 69.49, H 4.39.

Preparation of 9-(*p*-tolylselanyl)anthracene (1d): A similar method to that desribed for the preparation of **1a** was used. Compound **1d** was isolated in 75% yield as yellow needles. M.p. 144.8–145.7 °C; ^{1}H NMR (300 MHz, $CDCl_3$, TMS): δ = 2.17 (s, 3H), 6.85 (d, J = 7.9 Hz, 2H), 6.99 (d, J = 8.3 Hz, 2H), 7.54–7.55 (m, 4H), 8.00 (dd, J = 1.8, 7.6 Hz, 2H), 8.54-(s, 1H), 8.89 ppm (ddd, J = 1.0, 2.3, 7.9 Hz, 2H); ^{13}C NMR (75 MHz, $CDCl_3$, TMS): δ = 20.9, 125.4, 127.0, 128.9, 129.3, 129.5, 129.7, 129.9, 130.0 131.9, 132.3, 135.1, 135.6 ppm; ^{77}Se NMR (57 MHz, $CDCl_3$, MeSeMe): δ = 242.4 ppm; elemental analysis calcd (%) for $C_{21}H_{16}Se$: C 72.62, H 4.64; found: C 72.76, H 4.57.

Preparation of 9-(*p*-fluorophenylselanyl)anthracene (1e): A similar method to that desribed for the preparation of **1a** was used. Compound **1e** was isolated in 26% yield as yellow needles. M.p. 112.5–113.4 °C; ^{1}H NMR (300 MHz, $CDCl_3$, TMS): δ = 6.75 (dd, J = 4.5, 9.0 Hz, 2H), 7.06 (dd, J = 4.5, 6.0 Hz, 2H), 7.45–7.56 (m, 4H), 8.01 (d, J = 7.8 Hz, 2H), 8.55 (s, 1H), 8.85 ppm (d, J = 8.7 Hz, 2H); ^{13}C NMR (75 MHz, $CDCl_3$, TMS): δ = 116.2 (^2J(F,C) = 21.7 Hz), 125.5, 127.0, 127.2, 127.8 (^4J(F,C) = 3.3 Hz), 128.9, 129.3 (^3J(Se,C) = 9.5 Hz), 130.3, 131.0 (^3J(F,C) = 7.6, ^2J(Se,C) = 13.6 Hz), 131.9, 134.9 (^3J(Se,C) = 5.6 Hz), 161.5 ppm (^1J(F,C) = 245.2 Hz); ^{77}Se NMR (57 MHz, $CDCl_3$, MeSeMe): δ = 245.4 ppm (^5J(Se,F) = 6.2 Hz); elemental analysis calcd (%) for $C_{20}H_{13}FSe$: C 68.38, H 3.73; found: C 68.23, H 3.70.

Preparation of 9-(*p*-chlorophenylselanyl)anthracene (1f): A similar method to that desribed for the preparation of **1a** was used. Compound **1f** was isolated in 76% yield as yellow needles: M.p. 167.6–168.3 °C; ^{1}H NMR (300 MHz, $CDCl_3$, TMS): δ = 6.96–7.02 (m, 4H), 7.46–7.56 (m, 4H), 8.03 (dd, J = 2.8, 7.2 Hz, 2H), 8.59 (s, 1H), 8.81 ppm (dd, J = 2.3, 7.5 Hz, 2H); ^{13}C NMR (75 MHz, $CDCl_3$, TMS): δ = 122.4, 125.6, 127.1, 127.2, 127.6, 128.6, 128.8, 129.4, 130.6, 132.2, 133.3 (^2J(Se,C) = 11.6 Hz), 134.3 ppm; ^{77}Se NMR (57 MHz, $CDCl_3$, MeSeMe): δ = 250.5 ppm; elemental analysis calcd (%) for $C_{20}H_{13}ClSe$: C 65.32, H 3.56; found: C 65.43, H 3.49.

Preparation of 9-(*p*-Bromophenylselanyl)anthracene (1g): A similar method to that desribed for the preparation of **1a** was used. Compound **1g** was isolated in 69% yield as yellow needles. M.p. 180.4–181.0 °C; ^{1}H NMR (300 MHz, $CDCl_3$, TMS): δ = 6.91 (d, J = 8.5 Hz, 2H), 7.15 (d, J = 8.5 Hz, 2H), 7.47–7.57 (m, 4H), 8.04 (dd, J = 2.7, 6.9 Hz, 2H), 8.60 (s, 1H), 8.81 ppm (dd, J = 2.7, 6.9 Hz, 2H); ^{13}C NMR (75 MHz, $CDCl_3$, TMS): δ = 119.6, 125.6, 126.0, 127.4, 129.0, 129.1, 130.5, 130.6, 131.9, 132.1, 132.5, 135.0 ppm; ^{77}Se NMR (57 MHz, $CDCl_3$, MeSeMe): δ = 250.6 ppm; elemental analysis calcd (%) for $C_{20}H_{13}BrSe$: C 58.28, H 3.18; found: C 58.35, H 3.09.

Preparation of 9-[*p*-(ethoxycarbonyl)phenylselanyl]anthracene (1h): Under an argon atmosphere, 9-bromoanthracene (1.00 g, 3.89 mmol) was dissolved in dry diethyl ether (50 mL) and the solution was added to a flask that contained magnesium (0.10 g, 4.11 mmol) and dry diethyl ether (5 mL). The resulting solution was refluxed for 2 h. Selenium powder (0.30 g, 3.80 mmol) was then added and the mixture was refluxed for 2 h. Then a solution of diazonium, which was prepared from *p*-ethoxycarbonyl aniline (1.93 g, 11.7 mmol) in water (30 mL), was added dropwise . The mixture was heated to 40 °C for 30 min, and benzene (100 mL) was added. The organic layer was separated and was washed with water, 10% aqueous solution of sodium hydroxide, saturated aqueous solution of sodium bicarbonate, and brine. Then the solution was dried over sodium sulfate, evaporated, and dried in vacuo. The crude product was purified by column chromatography (SiO_2, hexane) to give **1h** as yellow needles. Yield: 5%, m.p. 148.0–149.0 °C; ^{1}H NMR (300 MHz, $CDCl_3$, TMS): δ = 1.33 (t, J = 7.2 Hz, 3H), 4.30 (q, J = 7.2 Hz, 2H), 7.22 (d, J = 8.6 Hz, 2H), 7.79 (d, J = 8.6 Hz, 2H), 7.49–7.59 (m, 4H), 8.04–8.10 (m, 2H), 8.65(s, 1H), 8.69–8.76 ppm (m, 2H); ^{13}C NMR (75 MHz, $CDCl_3$, TMS): δ = 14.8, 60.8, 125.5, 127.0, 127.2, 128.2, 128.9, 129.1, 129.3, 130.3, 130.6, 131.9, 134.9, 139.8, 165.6 ppm; ^{77}Se NMR (57 MHz, $CDCl_3$, MeSeMe): δ = 265.2 ppm; elemental analysis calcd (%) for $C_{23}H_{18}O_2Se$: C 68.15, H 4.48; found: C 68.35, H 4.53.

Preparation of 9-[*p*-cyanophenylselanyl]anthracene (1i): A similar method to that desribed for the preparation of **1a** was used. Compound **1i** was isolated in 83% yield as yellow needles. M.p. 163.1–164.0 °C; ^{1}H NMR (300 MHz, $CDCl_3$, TMS): δ = 7.05 (d, J = 8.6 Hz, 2H), 7.28 (d, J = 8.6 Hz, 2H), 7.49–7.59 (m, 4H), 8.04–8.10 (m, 2H), 8.65 (s, 1H), 8.69–

 © 2006 Wiley-VCH Verlag GmbH & Co. KGaA, Weinheim

8.76 ppm (m, 2H); ^{13}C NMR (75 MHz, $CDCl_3$, TMS): δ = 108.8, 118.9, 124.3, 125.8, 127.8, 128.7, 129.1, 130.5, 131.1, 131.9, 132.3, 135.1, 141.5 ppm; ^{77}Se NMR (57 MHz, $CDCl_3$, MeSeMe): δ = 275.2 ppm; elemental analysis calcd (%) for $C_{21}H_{13}NSe$: C 70.40, H 3.66, N 3.91; found: C 70.38, H 3.69, N 3.89.

Preparation of 9-[*p*-nitrophenylselanyl]anthracene (1j): Under an argon atmosphere, 9-bromoanthracene (1.00 g, 3.89 mmol) was dissolved in of dry diethyl ether (50 mL) and the solution was added to a flask that contained magnesium (0.10 g, 4.11 mmol) and dry diethyl ether (5 mL). The solution was refluxed for 2 h. Selenium powder (0.30 g, 3.80 mmol) was then added. Then the reaction mixture was refluxed for 2 h. Then *p*-iodonitrobenzen (0.97 g, 3.90 mmol) and ethanol (50 mL) was added, and the resulting mixture was refluxed for 2 h. Then the mixture was poured into ice water. The precipitated solid was flitted and dried in vacuo. The crude product was purified by column chromatography (SiO_2, hexane) to give **1j** as yellow needles. Yield: 72%, m.p. 150.0–150.8°C; ^{1}H NMR (300 MHz, $CDCl_3$, TMS): δ = 7.09 (d, J = 9.1 Hz, 2H), 7.51–7.58 (m, 4H), 7.88 (d, J = 9.1 Hz, 2H), 8.08 (dd, J = 2.2, 9.7 Hz, 2H), 8.67 (s, 1H), 8.72 ppm (dd, J = 2.2, 9.6 Hz, 2H); ^{13}C NMR (75 MHz, $CDCl_3$, TMS): δ = 124.0, 124.2, 125.8, 127.8, 128.4, 128.6, 129.2, 131.3, 132.0, 135.1, 144.3, 145.8 ppm; ^{77}Se NMR (57 MHz, $CDCl_3$, MeSeMe): δ = 279.3; elemental analysis calcd (%) for $C_{20}H_{13}NO_2Se$: C 63.50, H 3.46, N 3.70; found: C 63.36, H 3.42, N 3.74.

Preparation of 1-(phenylselanyl)anthraquinone (2a): Sodium hydride (0.07 g, 3.00 mmol) was added under an argon atmosphere to a solution of diphenyl diselenide (0.31 g, 1.00 mmol) in DMF (50 mL); the resulting micxture was then heated to 119.0–120.0°C. A solution of 1-chloroanthraquinone (0.24 g, 1.00 mmol) in DMF (30 mL) and CuI (1.14 g, 6.00 mmol) were added to the solution and stirring was continued for 2 h at 100°C. After pouring into ice water, the precipitate was filtrated. After usual workup, the crude product was subjected to chromatography on silica gel that was covered with a basic alumina layer on the top and recrystallized from ethanol/chloroform. Compound **2a** was isolated in 88% yield as dark red prisms. M.p. 181.2–182.9°C; ^{1}H NMR (300 MHz, $CDCl_3$, TMS): δ = 7.26 (dd, J = 1.1, 8.1 Hz, 1H), 7.41 (d, J = 7.8 Hz, 1H), 7.43–7.54 (m, 3H), 7.75 (dd, J = 1.7, 7.6 Hz, 2H), 7.80 (dd, J = 1.8, 7.2 Hz, 1H), 7.82 (dd, J = 1.8, 7.3 Hz, 1H), 8.19 (dd, J = 1.1, 7.5 Hz, 1H), 8.28 (dd, J = 2.2, 7.0 Hz, 1H), 8.38 ppm (dd, J = 2.2, 7.0 Hz, 1H); ^{13}C NMR (100 MHz, $CDCl_3$, TMS): δ = 124.8, 127.0, 127.4, 129.1, 129.5, 129.6, 129.9, 132.7, 132.8, 133.6, 133.9, 134.2, 135.4, 137.5, 143.0, 182.9, 183.7 ppm; ^{77}Se NMR (57 MHz, $CDCl_3$, MeSeMe): δ = 512.3 ppm; elemental analysis calcd (%) for $C_{20}H_{12}O_2Se$: C 66.13, H 3.33, found: C 66.32, H 3.15.

Preparation of 1-[(*N*,*N*'-dimethylamino)phenylselanyl]anthraquinone (2b): A similar method to that desribed for the preparation of **2a** was used. Compound **2b** was isolated in 89% yield as dark violet prisms. M.p. 288.5–289.5°C; ^{1}H NMR (300 MHz, $CDCl_3$, TMS): δ = 3.03 (s, 6H), 6.76 (d, J = 9.0 Hz, 2H), 7.36–7.40 (m, 2H), 7.54 (d, J = 8.8 Hz, 2H), 7.77 (dd, J = 1.7 and 7.3 Hz, 1H), 7.78 (dd, J = 1.8, 7.3 Hz, 1H), 8.10 (dd, J = 3.0, 5.9 Hz, 1H), 8.27 (dd, J = 2.0, 7.0 Hz, 1H), 8.38 ppm (dd, J = 2.0, 7.0 Hz, 1H); ^{13}C NMR (100 MHz, $CDCl_3$, TMS): δ = 40.2, 100.7, 113.6, 114.2, 124.6, 127.0, 127.5, 132.5, 133.0, 133.7, 134.1, 134.2, 134.5, 135.6, 138.6, 145.1, 151.3, 183.2, 183.7 ppm; ^{77}Se NMR (57 MHz, $CDCl_3$, MeSeMe): δ = 492.8 ppm; elemental analysis calcd (%) for $C_{22}H_{17}NO_2Se$: C 65.03, H 4.22, N 3.45; found: C 65.12, H 4.15, N 3.33.

Preparation of 1-(*p*-anisyl)anthraquinone (2c): A similar method to that desribed for the preparation of **2a** was used. Compound **2c** was isolated in 72% yield as dark red prisms. M.p. 240.6–241.5°C; ^{1}H NMR (300 MHz, $CDCl_3$, TMS): δ = 3.89 (s, 3H), 7.00 (d, J = 8.8 Hz, 2H), 7.28 (dd, J = 1.1, 8.3 Hz, 1H), 7.43 (t, J = 8.3 Hz, 1H), 7.64 (d, J = 8.8 Hz, 2H), 7.81 (dd, J = 1.8, 7.2 Hz, 1H), 7.83 (dd, J = 1.7, 7.2 Hz, 1H), 8.13 (dd, J = 1.3, 7.4 Hz, 1H), 8.30 (dd, J = 2.2, 6.8 Hz, 1H), 8.40 ppm (dd, J = 2.0, 7.0 Hz, 1H); ^{13}C NMR (75 MHz, $CDCl_3$, TMS): δ = 55.4, 115.7, 119.5, 124.8, 127.0, 127.5, 129.7, 132.7, 132.8, 133.7, 133.9, 134.2, 134.3, 135.5, 139.0 (^2J(Se,C) = 10.3 Hz), 143.9, 160.9, 183.1, 183.8 ppm; ^{77}Se NMR (57 MHz, $CDCl_3$, MeSeMe): δ = 497.3 ppm; elemental analysis calcd (%) for $C_{21}H_{14}O_3Se$: C 64.13, H 3.59; found: C 64.32, H 3.65.

Preparation of 1-(*p*-tolylselanyl)anthraquinone (2d): A similar method to that desribed for the preparation of **2a** was used. Compound **2d** was isolated in 76% yield as dark red prisms. M.p. 243.2–244.1°C; ^{1}H NMR (300 MHz, $CDCl_3$, TMS): δ = 2.45 (s, 3H), 7.23–7.32 (m, 3H), 7.41 (t, J = 8.6 Hz, 1H), 7.62 (d, J = 8.3 Hz, 2H), 7.81 (dd, J = 1.8, 7.2 Hz, 1H), 7.82 (dd, J = 1.8, 7.5 Hz, 1H), 8.13 (dd, J = 1.3, 7.2 Hz, 1H), 8.30 (dd, J = 2.2, 6.8 Hz, 1H), 8.39 ppm (dd, J = 2.6, 6.8 Hz, 1H); ^{13}C NMR (75 MHz, $CDCl_3$, TMS): δ = 21.4, 124.8, 125.5, 127.0, 127.5, 129.7, 130.8, 132.7, 132.8, 133.7, 133.9, 134.3, 134.3, 135.5, 137.4 (^2J(Se,C) = 9.9 Hz), 139.7, 143.5, 183.0, 183.7 ppm; ^{77}Se NMR (57 MHz, $CDCl_3$, MeSeMe): δ = 503.4 ppm; elemental analysis calcd (%) for $C_{21}H_{14}O_2Se$: C 66.85, H 3.74; found: C 66.82, H 3.61.

Preparation of 1-(*p*-Fluorophenylselanyl)anthraquinone (2e): A similar method to that desribed for the preparation of **2a** was used. Compound **2e** was isolated in 76% yield as orange prisms. M.p. 228.4–229.2°C; ^{1}H NMR (300 MHz, $CDCl_3$, TMS): δ = 7.16 (t, J = 5.5, 8.8 Hz, 2H), 7.22 (dd, J = 1.1, 8.3 Hz, 1H), 7.44 (t, J = 7.8 Hz, 1H), 7.72 (dd, J = 5.5, 8.8 Hz, 2H), 7.77–7.87 (m, 2H), 8.14 (dd, J = 1.3, 7.5 Hz, 1H), 8.30 (dd, J = 2.4, 6.8 Hz, 1H), 8.38 ppm (dd, J = 2.2, 6.8 Hz, 1H); ^{13}C NMR (75 MHz, $CDCl_3$, TMS): δ = 117.3 (^2J(F,C) = 21.3 Hz), 124.0 (^4J(F,C) = 3.7 Hz), 125.0, 127.1, 127.5, 129.6, 132.7, 132.9, 133.6, 134.0, 134.4, 135.5, 139.6 (^3J-(F,C) = 8.3 Hz, ^2J(Se,C) = 8.1 Hz), 140.0, 142.9, 163.8 (^1J(F,C) = 249.8 Hz), 182.9, 183.8 ppm; ^{77}Se NMR (57 MHz, $CDCl_3$, MeSeMe): δ = 502.2 ppm (^5J(Se,F) = 4.0 Hz); elemental analysis calcd (%) for $C_{20}H_{11}FO_2Se$: C 63.01, H 2.91; found: C 62.83, H 2.94.

Preparation of 1-(*p*-Chlorophenylselanyl)anthraquinone (2f). A similar method to that desribed for the preparation of **2a** was used. Compound **2f** was isolated in 76% yield as orange prisms. M.p. 247.0–247.9°C; ^{1}H NMR (300 MHz, $CDCl_3$/TMS): δ = 7.25 (dd, J = 1.1, 8.3 Hz, 1H), 7.44 (d, J = 8.4 Hz, 2H), 7.45 (t, J = 6.5 Hz, 1H), 7.68 (d, J = 8.3 Hz, 2H), 7.77–7.87 (m, 2H), 8.15 (dd, J = 1.1, 7.5 Hz, 1H), 8.30 (dd, J = 2.4, 6.8 Hz, 1H), 8.39 ppm (dd, J = 2.4, 6.8 Hz, 1H); ^{13}C NMR (75 MHz, $CDCl_3$/TMS): δ = 125.1, 127.1, 127.4, 127.5, 129.7, 130.2, 132.8, 133.0, 133.0, 133.6, 134.1, 134.4, 135.5 (^2J(Se,C) = 3.1 Hz), 136.2, 138.9 (^2J(Se,C) = 10.4 Hz), 142.5, 182.9, 183.8 ppm; ^{77}Se NMR (57 MHz, $CDCl_3$/MeSeMe): δ = 505.3 ppm; elemental analysis calcd (%) for $C_{20}H_{11}ClO_2Se$: C 60.40, H 2.79; found: C 60.42, H 2.70.

Preparation of 1-(*p*-Bromophenylselanyl)anthraquinone (2g). A similar method to that desribed for the preparation of **2a** was used. Compound **2g** was isolated in 76% yield as orange prisms. M.p. 243.9–244.8°C; ^{1}H NMR (300 MHz, $CDCl_3$/TMS): δ = 7.25 (dd, J = 1.1, 7.9 Hz, 1H), 7.45 (t, J = 7.9 Hz, 1H), 7.57–7.63 (m, 4H), 7.78–7.88 (m, 2H), 8.15 (dd, J = 1.3, 7.6 Hz, 1H), 8.30 (dd, J = 2.6, 6.6 Hz, 1H), 8.39 ppm (dd, J = 2.4, 6.8 Hz, 1H); ^{13}C NMR (75 MHz, $CDCl_3$/TMS): δ = 124.4, 125.1, 127.1, 127.5, 128.0, 129.7, 132.8, 133.0, 133.2, 133.6, 134.0, 134.0, 134.3, 135.8, 139.1 (^2J(Se,C) = 10.2 Hz), 142.3, 182.8, 183.8 ppm; ^{77}Se NMR (57 MHz, $CDCl_3$/MeSeMe): δ = 505.9 ppm; elemental analysis calcd (%) for $C_{20}H_{11}BrO_2Se$: C 54.33, H 2.51; found: C 54.07, H 2.43.

Preparation of 1-[*p*-(Ethoxycarbonyl)phenylselanyl]anthraquinone (2h): A similar method to that desribed for the preparation of **2a** was used. Compound **2h** was isolated in 66% yield as orange prisms. M.p. 234.0–234.9°C; ^{1}H NMR (300 MHz, $CDCl_3$/TMS): δ = 1.33 (t, J = 7.2 Hz, 3H), 4.30 (q, J = 7.2 Hz, 2H), 7.21 (dd, J = 1.1, 8.1 Hz, 1H), 7.22 (d, J = 8.6 Hz, 2H), 7.48 (t, J = 7.9 Hz, 1H), 7.79 (d, J = 8.6 Hz, 2H),7.82–7.87 (m, 2H), 8.19 (dd, J = 1.1, 8.4 Hz, 1H), 8.29–8.34 (m, 1H), 8.36–8.41 ppm (m, 1H); ^{13}C NMR (75 MHz, $CDCl_3$, TMS): δ = 14.2, 61.2, 125.2, 127.2, 127.5, 128.2, 129.4, 132.7, 133.1, 133.2, 133.4, 134.0, 134.3, 134.5, 135.5, 135.8, 137.9, 141.1, 166.2, 182.7, 183.9 ppm; ^{77}Se NMR (57 MHz, $CDCl_3$/MeSeMe): δ = 512.3 ppm; elemental analysis calcd (%) for $C_{23}H_{16}O_4Se$: C 63.46, H 3.70; found: C 63.48, H 3.65.

Preparation of 1-(*p*-Cyanophenylselanyl)anthraquinone (2i): A similar method to that desribed for the preparation of **2a** was used. Compound **2i** was isolated in 40% yield as orange prisms. M.p. 279.6–280.9°C; ^{1}H NMR (300 MHz, $CDCl_3$/TMS): δ = 7.20 (dd, J = 1.1, 8.1 Hz, 1H), 7.48 (t, J = 7.9 Hz, 1H), 7.74 (d, J = 8.4 Hz, 2H), 7.82–7.87 (m, 2H), 7.88 (d, J = 8.4 Hz, 2H), 8.19 (dd, J = 1.1, 8.4 Hz, 1H), 8.29–8.34 (m, 1H), 8.36–8.41 ppm (m, 1H); ^{13}C NMR (75 MHz, $CDCl_3$/TMS): δ = 113.3, 118.3, 125.4, 127.2, 127.5, 129.8 (^2J(Se,C) = 10.6 Hz), 132.7, 133.1, 133.2, 133.4,

 © 2006 Wiley-VCH Verlag GmbH & Co. KGaA, Weinheim

134.0, 134.3, 134.5, 135.5, 135.8, 137.9, 141.1, 182.7, 183.9 ppm; ^{77}Se NMR (57 MHz, $CDCl_3$/MeSeMe): $\delta = 520.5$ ppm; elemental analysis calcd (%) for $C_{21}H_{11}NO_2Se$: C 64.96, H 2.86, N 3.61; found: C 64.67, H 2.95, N 3.63.

Preparation of 1-(*p*-Nitrophenylselanyl)anthraquinone (2j). A similar method to that desribed for the preparation of **2a** was used. Compound **2j** was isolated in 70% yield as orange prisms. M.p. 298.0–299.0 °C; ^{1}H NMR (300 MHz, $CDCl_3$/TMS): $\delta = 7.23$ (dd, $J = 1.1$, 8.6 Hz, 1H), 7.48 (t, $J = 7.9$ Hz, 1H), 7.85 (m, 2H), 7.94 (d, $J = 8.6$ Hz, 2H), 8.20 (dd, $J = 1.1$, 7.7 Hz, 1H), 8.30 (d, $J = 8.6$ Hz, 2H), 8.32 (dd, $J = 1.1$, 7.4 Hz, 1H), 8.39 ppm (dd, $J = 1.1$, 7.4 Hz, 1H); ^{13}C NMR (75 MHz, $CDCl_3$, TMS): $\delta =$ 123.6, 125.2, 127.1, 127.5, 129.4, 133.1, 133.2, 133.4, 134.0, 134.3, 134.5, 135.5, 135.8, 137.9, 143.8, 146.1, 182.7, 183.9 ppm; ^{77}Se NMR (57 MHz, $CDCl_3$/MeSeMe): $\delta = 514.8$ ppm; elemental analysis calcd (%) for $C_{20}H_{11}NO_4Se$: C 58.84, H 2.72, N 3.43; found: C 58.99, H 2.89, N 3.61.

X-ray structural determination of 1c and 2a: The yellow crystals of **1c** and the orange crystals of **2a** were grown by slow evaporation of a solution of the sample in dichloromethane/benzene or benzene/hexane solvent mixtures at room temperature. The intensity data were collected on a Rigaku AFC5R four-circle diffractometer with graphite-monochromated $Mo_{K\alpha}$ radiation ($\lambda = 0.71069$ Å) for **1c** and **2a**. The structures of **1c** and **2a** were solved by heavy-atom Patterson methods, PATTY,[45] and expanded by using Fourier techniques, DIRDIF94.[46] All the non-hydrogen atoms were refined anisotropically. Hydrogen atoms were included but not refined. The final cycle of full-matrix least-squares refinement was based on a total of 4232 reflections for **1c** and on 2560 for **2a** with 415 and 212 [$I > 1.50\sigma(I)$] observed reflections for **1c** and **2a**, respectively. Variable parameters and converged with unweighted and weighted agreement factors of $R = (\Sigma||F_o| - |F_c||)/\Sigma|F_o|$ and $R_\omega = \{\Sigma\omega(|F_o| - |F_c|)^2/\Sigma\omega F_o^2\}^{1/2}$ were used. For least squares, the function minimized was $\Sigma\omega(|F_o| - |F_c|)^2$, in which $w = (\sigma_2^c|F_o| + p^2|F_o|^2/4)^{-1}$. Crystallographic details are given in the Supporting Information. CCDC-283618 and CCDC-283619 contain the supplementary crystallographic data for this paper. These data can be obtained free of charge from The Cambridge Crystallographic Data Centre via www.ccdc.cam.ac.uk/data_request/cif.

MO Calculations: Quantum chemical (QC) calculations were performed by using a Silent-SCC T2 (Itanium2) computer with the 6–311+G(3df) basis sets for Se and 6–311+G(3d,2p) for other nuclei of the Gaussian 03 program.[29] Calculations were performed on **4**–**6** in pl and pd confomations at the density functional theory (DFT) level of the Becke three-parameter hybrid functionals combined with the Lee-Yang-Parr correlation functional (B3LYP). Absolute magnetic shielding tensors of Se nuclei (σ(Se)) were calculated based on the gauge-independent atomic orbital (GIAO) method, applying on the optimized structures with the same method. A utility program (NMRANAL-NH98G) was prepared to carry out decomposing the magnetic shieldings, based on the Gaussian 98.[15] The program was applied to SeH_2, **4**(pl), **4**(pd) (Y = H, NH_2, Me, F, CN, and NO_2) **5** (pl), **5**(pd), and **6a** (Y = H) to evaluate the contributions separately from each molecular orbital (ψ_i) and each $\psi_i \rightarrow \psi_j$ transition, in which ψ_i and ψ_j denote occupied and unoccupied molecular orbitals, respectively.

Structures of **1a**–**3a** in various conformers were also optimized with the B3LYP/6–311+G(d,p) method. The frequency analysis was also performed.

Acknowledgements

This work was partially supported by a Grant-in-Aid for Scientific Research (No. 16550038) from the Ministry of Education, Culture, Sports, Science, and Technology, Japan.

[1] a) *Organic Selenium Compounds: Their Chemistry and Biology* (Eds.: D. L. Klayman, W. H. H. Günther), Wiley, New York, **1973**; b) *The Chemistry of Organic Selenium and Tellurium Compounds, Vols. 1 and 2* (Eds.: S. Patai, Z. Rappoport), Wiley, New York, **1986**; c) *Organic Selenium Chemistry* (Ed.: D. Liotta), Wiley-Interscience, New York, **1987**; d) *Organoselenium Chemistry, A practical Approach* (Ed.: T. G. Back), Oxford University Press, Oxford, **1999**; e) "Organoselenium Chemistry: Modern Developments in Organic Synthesis": *Top. Curr. Chem.* **2000**, *208*, whole volume.

[2] a) W. MacFarlane, R. J. Wood, *J. Chem. Soc. Dalton Trans.* **1972**, 13, 1397–1401; b) H. Iwamura, W. Nakanishi, *Yuki Gosei Kagaku Kyokaishi (J. Synth. Org. Chem. Jpn.)* **1981**, *39*, 795–804; c) *The Chemistry of Organic Selenium and Tellurium Compounds, Vol. 1* (Eds.: S. Patai, Z. Rappoport), Wiley, New York, **1986**, Chapter 6; d) *Compilation of Reported ^{77}Se NMR Chemical Shifts* (Eds.: T. M. Klapotke, M. Broschag), Wiley, New York, **1996**; e) H. Duddeck, *Prog. Nucl. Magn. Reson. Spectrosc.* **1995**, *27*, 1–323.

[3] a) S. Gronowitz, A. Konar, A.-B. Hörnfeldt, *Org. Magn. Reson.* **1977**, *9*, 213–217; b) G. P. Mullen, N. P. Luthra, R. B. Dunlap, J. D. Odom, *J. Org. Chem.* **1985**, *50*, 811–816; c) G. A. Kalabin, D. F. Kushnarev, V. M. Bzesovsky, G. A. Tschmutova, *Org. Magn. Reson.* **1979**, *12*, 598–604; d) G. A. Kalabin, D. F. Kushnarev, T. G. Mannafov, *Zh. Org. Khim.* **1980**, *16*, 505–512; e) W. Nakanishi, S. Hayashi, T. Uehara, *Eur. J. Org. Chem.* **2001**, *2001*, 3933–3943.

[4] a) S. Hayashi, W. Nakanishi, *J. Org. Chem.* **1999**, *64*, 6688–6696; b) W. Nakanishi, S. Hayashi, H. Yamaguchi, *Chem. Lett.* **1996**, 947–948; c) W. Nakanishi, S. Hayashi, A. Sakaue, G. Ono, Y. Kawada, *J. Am. Chem. Soc.* **1998**, *120*, 3635–3640; d) W. Nakanishi, S. Hayashi, *J. Org. Chem.* **2002**, *67*, 38–48.

[5] a) W. Nakanishi, S. Hayashi, *Chem. Lett.* **1998**, 523–524; b) W. Nakanishi, S. Hayashi, *J. Phys. Chem. A* **1999**, *103*, 6074–6081.

[6] D. H. R. Barton, M. B. Hall, Z. Lin, S. I. Parekh, J. Reibenspies, *J. Am. Chem. Soc.* **1993**, *115*, 5056–5059.

[7] a) *Encyclopedia of Nuclear Magnetic Resonance* (Eds.: D. M. Grant, R. K. Harris), Wiley, New York, **1996**; b) *Nuclear Magnetic Shieldings and Molecular Structure* (Ed.: J. A. Tossell), Kluwer Academic, Dordrecht, Boston, London, **1993**; c) *Calculation of NMR and EPR Parameters; Theory and Applications* (Eds.: M. Kaupp, M. Bühl, V. G. Malkin), Wiley-VCH, Weinheim, **2004**; d) *Spins in Chemistry* (Ed.: R. McWeeny), Academic Press, New York, **1970**; e) "A Tool for Chemistry": V. G. Markin, O. L. Malkina, L. A. Eriksson, in *Modern Density Functional Theory* (Eds.: J. M. Seminario, P. Politzer), Elsever, Amsterdam, **1994**; f) *Density Functional Methods in Chemistry and Material Science* (Ed.: M. Springborg), Wiley, New York, **1977**.

[8] a) R. Fukuda, M. Hada, H. Nakatsuji, *J. Chem. Phys.* **2003**, *118*, 1015–1026; b) R. Fukuda, M. Hada, H. Nakatsuji, *J. Chem. Phys.* **2003**, *118*, 1027–1035; c) S. Tanaka, M. Sugimoto, H. Takashima, M. Hada, H. Nakatsuji, *Bull. Chem. Soc. Jpn.* **1996**, *69*, 953–959; d) C. C. Ballard, M. Hada, H. Kaneko, H. Nakatsuji, *Chem. Phys. Lett.* **1996**, *254*, 170–178; e) H. Nakatsuji, M. Hada, H. Kaneko, C. C. Ballard, *Chem. Phys. Lett.* **1996**, *255*, 195–202; f) M. Hada, H. Kaneko, H. Nakatsuji, *Chem. Phys. Lett.* **1996**, *261*, 7–12.

[9] a) K. Kanda, H. Nakatsuji, T. Yonezawa, *J. Am. Chem. Soc.* **1984**, *106*, 5888–5892; b) *Molecular Quantum Mechanics*, 3rd ed. (Eds.: P. W. Atkins, R. S. Friedman), Oxford University Press, Oxford, New York, **1997**, Chapter 13.

[10] a) N. F. Ramsey, *Phys. Rev.* **1949**, *77*, 567; b) N. F. Ramsey, *Phys. Rev.* **1950**, *78*, 699–703; c) N. F. Ramsey, *Phys. Rev.* **1951**, *83*, 540–541; d) N. F. Ramsey, *Phys. Rev.* **1956**, *86*, 243–246; e) N. F. Ramsey, *Phys. Rev.* **1952**, *85*, 143–144; f) N. F. Ramsey, *Phys. Rev.* **1953**, *91*, 303–307.

[11] W. Nakanishi, S. Hayashi, T. Uehara, *J. Phys. Chem. A* **1999**, *103*, 9906–9912.

[12] The nonplanar and nonperpendicular conformer (np) is also important in some cases, for example, CC in 1-MeSe-8-$PhSeC_{10}H_6$.[11]

[13] The importance of relative conformations in the substituent effects between substituents and probe sites is pointed out. See for example, "Angular Dependence of Dipolar Substituent Effects": K. Bordwen, E. J. Grubbs, *Prog. Phys. Org. Chem.* **1993**, *19*, 183–224, and references therein.

[14] a) K. Wolinski, J. F. Hinton, P. Pulay, *J. Am. Chem. Soc.* **1990**, *112*, 8251–8260; b) K. Wolinski, A. Sadlej, *Mol. Phys.* **1980**, *41*, 1419–

 © 2006 Wiley-VCH Verlag GmbH & Co. KGaA, Weinheim

1430; c) R. Ditchfield, *Mol. Phys.* **1974**, *27*, 789–807; d) R. McWeeny, *Phys. Rev.* **1962**, *126*, 1028–1034; e) F. London, *J. Phys. Radium* **1937**, *8*, 397–409.

[15] Gaussian 98 (Revision A.11), M. J. Frisch, G. W. Trucks, H. B. Schlegel, G. E. Scuseria, M. A. Robb, J. R. Cheeseman, V. G. Zakrzewski, J. A. Montgomery, Jr., R. E. Stratmann, J. C. Burant, S. Dapprich, J. M. Millam, A. D. Daniels, K. N. Kudin, M. C. Strain, O. Farkas, J. Tomasi, V. Barone, M. Cossi, R. Cammi, B. Mennucci, C. Pomelli, C. Adamo, S. Clifford, J. Ochterski, G. A. Petersson, P. Y. Ayala, Q. Cui, K. Morokuma, P. Salvador, J. J. Dannenberg, D. K. Malick, A. D. Rabuck, K. Raghavachari, J. B. Foresman, J. Cioslowski, J. V. Ortiz, A. G. Baboul, B. B. Stefanov, G. Liu, A. Liashenko, P. Piskorz, I. Komaromi, R. Gomperts, R. L. Martin, D. J. Fox, T. Keith, M. A. Al-Laham, C. Y. Peng, A. Nanayakkara, M. Challacombe, P. M. W. Gill, B. Johnson, W. Chen, M. W. Wong, J. L. Andres, C. Gonzalez, M. Head-Gordon, E. S. Replogle, J. A. Pople, Gaussian, Pittsburgh PA, **2001**.

[16] While the torsional angle of C(1)-Se(1)-C(15)-C(16) in **1c**(S-A) is 174.8(4)°, that of C(22)-Se(2)-C(36)-C(37) in **1c**(S-B) is −155.2(5)°.[17] The latter must be deformed by the crystal packing effect. The main intermolecular short contacts around *p*-An in **1c**(S-A) (O···H_m and H_m···O) occur in the directions on the *p*-An plane with one of out of plane (H_{Me}···H_o). As the result, the structure of **1c**(S-A) is very close to that of **1c**(A:pl). However, those in **1c**(S-B) (C_m···H_{Me}, H_m···O, and H_o···H_2) occur mainly out of the plane direction with one of in plane (H_o···H_{Me}), which deforms the torsional angle from that in pure **1c**(A:pl) by about 25° in the crystal.

[17] The crystallographic data of **1c** and **2a** are collected in Table S1 of the Supporting Information and their selected interatomic distances, angles, and torsional angles in Table S2.

[18] The energies of structures **3a**(A:pl), **3a**(B:pd), and **3a**(B′:pd) were evaluated to be −3018.6354, −3018.6350, and −3018.6262 au, respectively, by the B3LYP/6–311+G(d,p) method.[29] The relative energies are 0.0, 1.1, and 24.2 kJ mol^{-1}, respectively. Structure **3a**(B′:pd) has an imaginary frequency ($\nu_1 = -38.9$ cm^{-1}), which corresponds to the motion to **3a**(A:pl). Structure **3a**(B′:pd) is predicted to be a transition state. The relative energies for the sum of electronic and thermal (Gibbs) free energies at 298 K of **3a**(A:pl), **3a**(B:pd), and **3a**(B′:pd) are 0.0, 0.0, and 29.1 kJ mol^{-1}, respectively.

[19] The energies of structures **1a**(A:pl) and **1a**(A:pd) were evaluated to be −3172.3034 and −3172.3005 au, respectively, by the B3LYP/6–311+G(d,p) method.[29] Structure **1a**(A:pl) is predicted to be more stable than **1a**(A:pd) by 7.6 kJ mol^{-1} on the energy surface. While all frequencies of **1a**(A:pl) are positive, those of **1a**(A:pd) contain one imaginary frequency of $\nu_1 = -20.6$ cm^{-1}. Structure **1a**(A:pd) is predicted to be a transition state. The sum of electronic and thermal (Gibbs) free energies at 298 K of **1a**(A:pl) and **1a**(A:pd) are −3172.0769 and −3172.0717 au, respectively. The difference is 13.7 kJ mol^{-1}.

[20] The p–π conjugation of the n_p(Se)–π(Ar) type plays an additional role to affect the stability of **1**(A:pl); cases in which Y is an acceptor stabilize **1**(A:pl) more effectively than cases in which Y is a donor (compare **3**(A:pl) versus **3**(B:pd)).[3e] Since Y=OMe is one of strong donors, the structure of **1c**(A:pl) strongly supports the global minimum of (A:pl) for **1**.

[21] The evaluated energies of **2a**(A:pl) and **2a**(B:pd) were −3321.5894 and −3321.6015 au, respectively, by the B3LYP/6–311+G(d,p) method.[29] Structure **2a**(B:pd) is more stable than **2a**(A:pl) by 31.8 kJ mol^{-1}. Structure **2a**(A:pl) is close to **2a**(A:np),[12] in which the Ph group is close to the O=C group.

[22] For hypervalent bonds, see, a) G. C. Pimentel, *J. Chem. Phys.* **1951**, *19*, 446–448 b) J. I. Musher, *Angew. Chem.* **1969**, *81*, 68–83; Angew. Chem. Int. Ed. Engl. **1969**, 8, 54–68; c) M. M. L. Chen, R. Hoffmann, *J. Am. Chem. Soc.* **1976**, *98*, 1647–1653; d) P. A. Cahill, C. E. Dykstra, J. C. Martin, *J. Am. Chem. Soc.* **1985**, *107*, 6359–6362; e) R. A. Hayes, J. C. Martin, *Sulfurane Chemistry, in Organic Sulfur Chemistry: Theoretical and Experimental Advances* (Eds.: F. Bernardi, I. G. Csizmadia, A. Mangini), Elsevier, Amsterdam, **1985**, Chapter 8; f) *Chemistry of Hypervalent Compounds* (Ed.: K.-y. Akiba), Wiley-VCH, Weinhaim, **1999**.

[23] If two nonbonded n_p(O)→σ*(Z–C) (Z=S and Se) 3c-4e interactions operate at the both sides of the n_p(O), extended hypervalent 5c-6e interactions are constructed. See, W. Nakanishi, S. Hayashi, N. Itoh, *Chem. Commun.* **2003**, *2003*, 124–125; W. Nakanishi, S. Hayashi, N. Itoh, *J. Org. Chem.* **2004**, *69*, 1676–1684; W. Nakanishi, S. Hayashi, T. Furuta, N. Itoh, Y. Nishina, M. Yamashita, Y. Yamamoto, *Phosphorus Sulfur Silicon Relat. Elem.* **2005**, *180*, 1351–1355.

[24] Details of the structure of **2** will be discussed with respect to the O···Se–C 3c-4e interaction elsewhere.

[25] The **1**(A:pl) and **2**(B:pd) structures are supported by the X-ray crystallographic analysis and QC calculations. These structures in crystals and in the gas phase will also exist in solution. The equilibrium with other conformers would not to be so severe in the solution for **1**(A:pl), since it is mainly in equilibrium with its duplicate. Structure **2**(B:pd) will be much more stable than other conformers. Observed δ(Se) values support the expectation.

[26] The 0.050 M $CDCl_3$ solutions were used for NMR measurements. However, the concentrations would be lower for the compounds of low solubility, such as **1j** and **2j** at 213 K.

[27] The temperature dependence of δ(Se) of MeSeMe in [D]chloroform (60% v/v) is reported to be about 2.5 ppm over the temperature range of 222–323 K. See N. P. Luthra, R. B. Dunlap, J. D. Odom, *J. Magn. Reson.* **1983**, *52*, 318–322.

[28] When the axes from the Gaussian 03[29] calulations were not the same as those shown in Scheme 3, they were interchanged so as to be those in Scheme 3 for convenience of discussion, if possible.

[29] Gaussian 03 (Revision B.05), M. J. Frisch, G. W. Trucks, H. B. Schlegel, G. E. Scuseria, M. A. Robb, J. R. Cheeseman, J. A. Montgomery, Jr. T. Vreven, K. N. Kudin, J. C. Burant, J. M. Millam, S. S. Iyengar, J. Tomasi, V. Barone, B. Mennucci, M. Cossi, G. Scalmani, N. Rega, G. A. Petersson, H. Nakatsuji, M. Hada, M. Ehara, K. Toyota, R. Fukuda, J. Hasegawa, M. Ishida, T. Nakajima, Y. Honda, O. Kitao, H. Nakai, M. Klene, X. Li, J. E. Knox, H. P. Hratchian, J. B. Cross, C. Adamo, J. Jaramillo, R. Gomperts, R. E. Stratmann, O. Yazyev, A. J. Austin, R. Cammi, C. Pomelli, J. W. Ochterski, P. Y. Ayala, K. Morokuma, G. A. Voth, P. Salvador, J. J. Dannenberg, V. G. Zakrzewski, S. Dapprich, A. D. Daniels, M. C. Strain, O. Farkas, D. K. Malick, A. D. Rabuck, K. Raghavachari, J. B. Foresman, J. V. Ortiz, Q. Cui, A. G. Baboul, S. Clifford, J. Cioslowski, B. B. Stefanov, G. Liu, A. Liashenko, P. Piskorz, I. Komaromi, R. L. Martin, D. J. Fox, T. Keith, M. A. Al-Laham, C. Y. Peng, A. Nanayakkara, M. Challacombe, P. M. W. Gill, B. Johnson, W. Chen, M. W. Wong, C. Gonzalez, J. A. Pople, Gaussian, Inc., Pittsburgh PA, **2003**.

[30] The torsional angle of $\phi = C_oC_iSeH$ in **4**(pd) is fixed at 90.0°, if **4**(pd) is not the C_s symmetry (e.g., Y=COOMe and OMe). Similarly, those of $\phi = C_oC_iSeC_{Me}$ and $\phi = C_iSeC_{Me}H$ in **5**(pd) are fixed at 90.0 and 180°, respectively, and those of $\phi = C_oC_iSeC_{i'}$ and $\phi = C_iSeC_{i'}C_{o'}$ in **6**(pd) are at 90.0 and 0°, respectively, when *p*-YC_6H_4Se is not the C_s symmetry.

[31] MolStudio R3.2 Rev 1.0, NEC Corporation, **1977–2003**.

[32] Evaluated values of σ^p(Se) and the components by the Gaussian 98 are sometimes substantially different from those by the Gaussian 03, although the structures are the same. The differences in $\sigma^p(Se)_{xx}$ and $\sigma^p(Se)_{yy}$ amount to 50 ppm or less for **4a**(pd) and **5a**(pd). They are very large for $\sigma^p(Se)_{xx}$ (−232.8 ppm) and $\sigma^p(Se)_{yy}$ (212.7 ppm) in **6a**. Axes of **6a** were bisected in Gaussian 98. Axes were chosen to be more close to those in **6**(pl).

[33] Chemical shifts have been discussed with parallel and perpendicular components. See reference [7].

[34] $\sigma^p(Se)_{xx}$, $\sigma^p(Se)_{yy}$, $\sigma^p(Se)_{zz}$, and σ^p(Se) of ψ_{13} are 0.1, −6.2, −0.2, and −2.1 ppm, respectively.

[35] The values are summed over ψ_i of the A″ symmetry for **4a**–**6a** of pl and pd, which are constructed by p_z(Se) and 3d(Se).

[36] Whereas $\sigma^p(Se)_{zz(zi)}$ of **4a**(pd) is almost zero, that of **4a**(pl) is −11 ppm. The non-zero nature of $\sigma^p(Se)_{zz(zi)}$ seems common in **4**(pl) (6–10 ppm), although not shown.

 © 2006 Wiley-VCH Verlag GmbH & Co. KGaA, Weinheim

[37] Calculations of σ(Se) for H_2Se, see, a) W. Kutzelnigg, U. Fleischer, C. van Wüllen, *Encyclopedia of Nuclear Magnetic Resonance, Vol. 7* (Eds.: D. M. Grant, R. K. Harris), Wiley, New York, **1996**, pp. 4284–4291; b) P. D. Ellis, J. D. Odom, A. S. Lipton, Q. Chen, J. M. Gulick, *Nuclear Magnetic Shieldings and Molecular Structure* (Ed.: J. A. Tossell), Kluwer Academic, Dordrecht, Boston, London, **1993**, pp. 539–555; c) P. J. Wilson, *Molecular Physics* **2001**, *99*, 363–367. Those for **4**(pl) and **4**(pd), see reference [5b].

[38] Details of the analysis of δ(Se) in SeH_2 and MeSeH will be reported elsewhere.

[39] DFT shieldings are deshielded in general, due to the underestimation of orbital energy differences, which leads to the overestimation of σ^p(Se).[37c] Therefore, σ^t(Se) of **4a**(pl), **4a**(pd), **5a**(pl), and **5a**(pd) were evaluated with the MP2/6-31+G(2d,p) method applying the GIAO method on the structures optimized with the MP2/6-31+G(3d,2p) method. The values are 1827.3, 1865.5, 1761.0, and 1708.7 ppm, respectively: σ^t of **4a**(pd) is predicted to be larger than that of **4a**(pl) by 38 ppm, whereas σ^t(Se) of **5a**(pd) is smaller than that of **5a**(pl) by 46 ppm. The results supports the orientational effects evaluated at the DFT level for **4a** and **5a**, although the basis sets are not the same.

[40] Interactions between n_p(Se) of $4p_z$(Se) and phenyl σ orbitals in **4a**(pd) must be weak due to large energy differences between $4p_z$(Se) and the σ orbitals. Long distances between them are also disadvantageous.

[41] The results may show that the $4p_y$(Se) orbital involved in the Se−C bond works effectively to shift downfield, whereas the $4p_x$(Se) orbital involved in the Se−H bond causes an upfield shift, when Y=H changes to non-H in **4**(pl).

[42] A similar trend is observed in **5**(pl) as in the case of **4**(pl), although the direction is reversed.

[43] $\sigma^p(Se)_{zz}$ is almost constant in the change of Y for both pl and pd of **4**–**6**. The small Y dependence of $\sigma^p(Se)_{zz}$ is reasonably explained by the main interaction of the $4p_z$(Se)–π(C_6H_4)–p_z(Y) type in pl, in which $4p_x$(Se) and $4p_y$(Se) do not take part in the interaction directly. The main interaction in pd is the σ(C_{Ar}SeX)–π(C_6H_4)–p_x(Y) (X= H or C) type, which modifies the contribution of $4p_x$(Se) and $4p_y$(Se) in the C_{Ar}SeX moiety. However, the results show that the interaction in pd affect the $\sigma^p(Se)_{xx}$ and $\sigma^p(Se)_{yy}$ parameters, but not the $\sigma^p(Se)_{zz}$.

[44] A very wide range of σ^p(Se) for **4**(pd) must be responsible for the results: The σ^p(Se) values for **4**(pd) were evaluated to be −2827, −1435, and −16155 ppm for Y=O^+, S^+, and Se^+, respectively. The corresponding values for **4**(pl) are −1976, −1841, and −1733 ppm, respectively.

[45] P. T. Beurskens, G. Admiraal, G. Beurskens, W. P. Bosman, S. Garcia-Granda, R. O. Gould, J. M. M. Smits, C. Smykalla, The DIRDIF program system, Technical Report of the Crystallography Laboratory, University of Nijmegen, The Netherlands, **1992**.

[46] P. T. Beurskens, G. Admiraal, G. Beurskens, W. P. Bosman, R. de Gelder, R. Israel, J. M. M. Smits, The DIRDIF-94 program system, Technical Report of the Crystallography Laboratory, University of Nijmegen, The Netherlands, **1994**.

Received: August 1, 2005
Revised: December 12, 2005
Published online: March 3, 2006

 © 2006 Wiley-VCH Verlag GmbH & Co. KGaA, Weinheim